

A Simultaneous Analysis of the Microwave, Submillimeterwave, Far Infrared, and Infrared–Microwave Two-Photon Transitions between the Ground and ν_2 Inversion–Rotation Levels of $^{14}\text{NH}_3$

Š. URBAN, V. ŠPIRKO, AND D. PAPOUŠEK

*The J. Heyrovský Institute of Physical Chemistry and Electrochemistry,
Czechoslovak Academy of Sciences, 160 00 Prague 6, Czechoslovakia*

J. KAUPPINEN

Department of Physics, University of Oulu, Finland

AND

S. P. BELOV, L. I. GERSHTEIN, AND A. F. KRUPNOV

Institute for Applied Physics, Academy of Sciences, Gorkii, USSR

Fourier transform infrared spectra of the inversion–rotation transitions have been measured with 0.010-cm^{-1} resolution between 40 and 300 cm^{-1} in the ground state and ν_2 excited states of $^{14}\text{NH}_3$. Submillimeterwave spectra of the inversion and inversion–rotation transitions in the ν_2 state of $^{14}\text{NH}_3$, including a few $\Delta k = \pm 3$ “perturbation-allowed” transitions, have been measured with microwave accuracy between 540 and 770 GHz. A simultaneous least-squares analysis of these data, the microwave ground-state transition frequencies, and the ν_2 infrared–microwave two-photon transition frequencies has been carried out. A theory of the $\Delta k = \pm 3n$ interactions in the ground and ν_2 excited states of ammonia (S. P. Belov, L. I. Gershtein, A. F. Krupnov, A. V. Maslovskij, Š. Urban, V. Špirko, and D. Papoušek, *J. Mol. Spectrosc.* **84**, 288–304 (1980)) has been used in the analysis. A set of the ground- and ν_2 -state molecular parameters has been obtained which describes the experimental data within the precision of the experiment. The “smoothed” values of transition frequencies can be used for calibration purposes with a precision better than $3 \times 10^{-5}\text{ cm}^{-1}$ in the submillimeterwave region, better than 10^{-3} cm^{-1} in the far-infrared region, and better than $1.5 \times 10^{-3}\text{ cm}^{-1}$ in the region $700\text{--}1200\text{ cm}^{-1}$.

I. INTRODUCTION

Precise knowledge of the frequencies of transitions between the ground and ν_2 inversion–rotation levels of ammonia is important; e.g., for astrophysical studies of the planetary and interstellar ammonia, in the investigation of optically pumped ammonia lasers, and for calibration purposes in the far- and medium-infrared regions.

In a previous paper (1) we measured the high-resolution infrared spectra of $^{14}\text{NH}_3$ in the region of the ν_2 , $2\nu_2$, and ν_4 bands and analyzed them using a

modified theory of the Coriolis and l -type interactions in ammonia; the theory of the $\Delta k = \pm 3n$ interactions was not introduced in that analysis. In a subsequent paper (2), we derived a theory of the $\Delta k = \pm 3n$ interactions, taking into account the large amplitude motion in ammonia, and applied it to the analysis of the submillimeterwave data on the inversion and inversion-rotation transitions in the ν_2 state of $^{14}\text{NH}_3$.

In the present paper we extended our measurements to the far-infrared region between 40 and 300 cm^{-1} (Fourier transform spectroscopy of the inversion-rotation transitions in the ground and ν_2 excited states of ammonia). We have also remeasured the spectra in the submillimeterwave region between 540 and 700 GHz (inversion and inversion-rotation transitions in the ν_2 excited state) mostly with microwave accuracy.

We combined the results of our previous measurements (1, 2), the present data, and precise literature data on the ground-state inversion transitions and the ν_2 band frequencies in a simultaneous least-squares analysis of the experimental data of three types: (i) microwave and far-infrared frequencies of transitions between the inversion and inversion-rotation energy levels in the ground state, (ii) frequencies of infrared-microwave two-photon transitions between the ground- and ν_2 -state energy levels, and (iii) submillimeterwave and far-infrared frequencies of transitions between the inversion and inversion-rotation levels in the ν_2 state.

In this analysis, the theory of the $\Delta k = \pm 3n$ interactions in ammonia (2) has been applied to the ground and excited ν_2 states. The experimental data used in the analysis were found to be internally consistent and extremely precise; ground-state and excited ν_2 -state molecular parameters of $^{14}\text{NH}_3$ have been obtained which describe these data within the accuracy of the experimental data. The "smoothed" values of the transition frequencies in the far- and medium-infrared regions obtained in this work are believed to be of accuracy sufficient for calibration purposes in the submillimeterwave, far-infrared, and medium-infrared regions.

II. EXPERIMENTAL DETAILS

The success in solving the problem outlined in Part I of this paper depends on the accuracy and internal consistency of the experimental data used in the analysis. As for the ground-state microwave data, we have used the frequencies of the pure inversion transitions of Poynter and Kakar (3) and Sinha and Smith (4) together with some frequencies of the inversion-rotation transitions measured by Gordy *et al.* (5) and Krupnov *et al.* (6).

For the ν_2 band transitions, infrared-microwave (7, 8) and infrared heterodyne measurements (9) have been combined with diode laser measurements calibrated as described in our previous paper (1).

The ground-state rotational and centrifugal distortion constants can be determined from the combination differences using the ν_2 -band frequencies. However, the very precise data on the ν_2 band (7-9) are not sufficiently complete to determine precise values of the higher-order centrifugal distortion constants.

The ground-state parameters could be determined from the inversion-rotation transitions which appear in the far-infrared region. The only available data on these transitions are those of Dowling (10) which, however, have only been measured with 0.08-cm^{-1} resolution and up to $J = 11$. We have therefore remeasured the far-infrared spectrum of ammonia in the range $35\text{--}278\text{ cm}^{-1}$ using a Fourier spectrometer recently built at the University of Oulu (11).

We have recorded the apodized Fourier spectra between 35 and 100 cm^{-1} using an $18\text{-}\mu\text{m}$ thick beamsplitter and between 100 and 278 cm^{-1} using an $8\text{-}\mu\text{m}$ thick beamsplitter. The total pressure of the sample in the cell for both spectra was $10.5 \times 10^{-3}\text{ Pa}$ (1.4 Torr). The sample, in liquid form before vaporization, comprises 25% NH_3 and 75% water (used for calibration). The resolution determined as a half-width of the weak lines was 0.014 cm^{-1} .

In order to resolve certain fine details, we have measured unapodized spectra in the corresponding spectral regions with 0.010-cm^{-1} resolution using an $18\text{-}\mu\text{m}$ beamsplitter. The total pressure of the sample in the cell was $8.25 \times 10^{-3}\text{ Pa}$ (1.1 Torr).

We have been able to assign the ground-state inversion-rotation transitions of $^{14}\text{NH}_3$ up to $J = 13$ (Table I). It can be seen that we have resolved almost completely the K structure of these transitions, except for a few transitions which are indicated in Table I.

We have also assigned the lines of the inversion-rotation transitions in the ν_2 excited state of $^{14}\text{NH}_3$ up to $J = 11$ (Table II). Many lines in our spectra could be assigned to the ground-state inversion-rotation spectrum of $^{15}\text{NH}_3$ occurring at natural abundance in the sample. Their frequencies agreed within the experimental accuracy with the recent Fourier spectra of $^{15}\text{NH}_3$ measured by Carlotti *et al.* (12), and they are not reported in our paper.

Typical parts of our apodized and unapodized Fourier spectra are shown in Figs. 1-5.

The basic source of information on the inversion and inversion-rotation transitions in the ν_2 excited state of ammonia are our submillimeterwave measurements reported in detail in our previous paper (2). In the present paper, we remeasured the spectra in the region $540\text{--}700\text{ GHz}$.

The high-sensitivity submillimeterwave spectrometer RAD (13, 14) at the Institute for Applied Physics of the Academy of Sciences USSR in Gorkii has been used with a system employing phase-sensitive frequency stabilization of the backward wave oscillator (15). The absolute accuracy of the measurements of frequencies is $\pm 10\text{ kHz}$ for lines with signal-to-noise ratios higher than 600; for the weakest lines (cf. Table III and Fig. 6) the experimental uncertainty can reach $\pm 0.5\text{ MHz}$. However, as we pointed out in our previous paper (2), the line centers of ammonia for transitions in the ν_2 excited state exhibit an anomalously large pressure dependence. In the present paper we measured at pressures of 53 Pa (0.4 Torr) of ammonia in the acoustic cell of the submillimeterwave spectrometer. The experimental uncertainty of the line frequencies taking into account this effect is therefore about $\pm 1\text{ MHz}$.

The results of measurements together with our previous submillimeterwave data are given in Tables III and V.

TABLE I

Inversion-Rotation Transition Wavenumbers (cm^{-1}) and Intensities ($\text{cm}^{-2} \text{atm}^{-1}$) of $^{14}\text{NH}_3$ in the Ground State^a

J	K	C	D	$(O-C)$ $\times 10^5$	I	J	K	C	D	$(O-C)$ $\times 10^5$	I
0	0	20.67324	---	---	0.	1	0	19.09648	19.09648 (1) ^b	0	0.14E+00
1	0	40.52312	---	---	0.11E+01	1	1	38.97687	---	---	0.
1	1	40.53622	---	---	0.42E+00	2	0	39.97337	39.97337 (100)	73	0.39E+00
2	0	60.32362	---	---	0.	2	1	58.82481	---	---	0.28E+01
2	1	60.33554	60.3407E (200)	125	0.13E+01	2	2	58.82738	---	---	0.12E+01
2	2	60.3877E	60.3870E (200)	-75	0.87E+00	3	0	58.83479	---	---	0.82E+00
3	0	80.05903	---	---	0.49E+01	3	1	78.62216	---	---	0.
3	1	80.07463	---	---	0.23E+01	3	2	78.62883	---	---	0.38E+01
3	2	80.13094	---	---	0.20E+01	3	3	78.64332	---	---	0.17E+01
3	3	80.22625	---	---	0.25E+01	4	0	78.67327	---	---	0.24E+01
4	0	99.70243	---	---	0.	4	1	98.34779	---	---	0.38E+01
4	1	99.72363	99.7237E (200)	8	0.30E+01	4	2	98.35691	---	---	0.01E+01
4	2	99.78754	99.7866E (100)	-94	0.28E+01	4	3	98.38407	---	---	0.27E+01
4	3	99.89152	99.8905E (200)	-98	0.17E+01	4	4	98.42871	---	---	0.45E+01
4	4	101.05020	101.0498E (200)	-40	0.15E+01	5	0	98.48937	---	---	0.14E+01
5	0	119.24982	---	---	0.64E+01	5	1	117.98182	---	---	0.
5	1	119.26938	---	---	0.32E+01	5	2	117.99437	117.9925E (200)	-167	0.31E+01
5	2	119.34059	119.3392E (100)	-129	0.30E+01	5	3	118.01815	118.0180E (200)	-45	0.30E+01
5	3	119.46077	119.4605E (100)	-27	0.56E+01	5	4	118.09173	118.0922E (200)	47	0.55E+01
5	4	119.53187	119.5320E (100)	32	0.21E+01	5	5	118.17594	118.1748E (100)	-113	0.23E+01
5	5	119.65607	119.6560E (80)	-8	0.15E+01	6	0	118.25146	118.2516E (200)	-16	0.15E+01
6	0	138.66995	---	---	0.	6	1	137.50508	---	---	0.54E+01
6	1	138.69586	138.6968E (200)	100	0.27E+01	6	2	137.52057	---	---	0.27E+01
6	2	138.77365	138.7732E (80)	-45	0.27E+01	6	3	137.54695	137.5572E (80)	25	0.27E+01
6	3	138.87437	138.8732E (100)	-282	0.32E+01	6	4	137.64434	---	---	0.51E+01
6	4	139.01088	139.0100E (200)	-187	0.24E+01	6	5	137.75051	137.7447E (200)	-60	0.24E+01
6	5	139.33808	139.3374E (80)	-68	0.21E+01	7	0	137.84481	---	---	0.20E+01
6	6	139.64843	139.6474E (200)	-102	0.27E+01	7	1	138.04795	138.0458E (200)	-215	0.27E+01
7	0	157.69076	---	---	0.40E+01	7	2	138.09292	---	---	0.
7	1	157.80766	---	---	0.20E+01	7	3	138.12778	138.1270E (100)	---	0.28E+01
7	2	158.07186	158.0718E (60)	0	0.20E+01	7	4	138.27334	138.2730E (100)	-33	0.20E+01
7	3	158.21453	158.2143E (100)	-22	0.41E+01	7	5	137.06446	137.0620E (200)	-265	0.40E+01
7	4	158.41203	158.4117E (200)	-32	0.21E+01	7	6	137.19430	137.1955E (200)	119	0.20E+01
7	5	158.67982	158.6786E (100)	-121	0.19E+01	7	7	137.35846	137.3579E (80)	-55	0.19E+01
7	6	159.01262	159.0112E (200)	-142	0.33E+01	7	8	137.55881	---	---	0.33E+01
7	7	159.41592	159.4159E (100)	-112	0.11E+01	7	9	137.78722	137.7888E (100)	-40	0.11E+01
8	0	177.13071	---	---	0.	8	1	176.14708	---	---	0.28E+01
8	1	177.13071	177.1296E (200)	-91	0.13E+01	8	2	176.16853	---	---	0.13E+01
8	2	177.25055	177.2514E (100)	128	0.38E+01	8	3	176.23266	176.2324E (100)	---	0.13E+01
8	3	177.37022	177.3683E (100)	-192	0.27E+01	8	4	176.34178	176.3415E (100)	-28	0.27E+01
8	4	177.50712	177.5054E (200)	-171	0.14E+01	8	5	176.48983	176.4884E (100)	-123	0.14E+01
8	5	177.60910	177.6100E (100)	90	0.14E+01	8	6	176.63139	---	---	0.14E+01
8	6	178.22262	178.2237E (100)	137	0.27E+01	8	7	176.91444	---	---	0.27E+01
8	7	178.65392	178.6538E (100)	-11	0.12E+01	8	8	177.18731	---	---	0.12E+01
8	8	179.07122	---	---	0.	8	9	177.49755	---	---	0.12E+01
9	0	196.08076	---	---	0.13E+01	9	1	195.23243	---	---	0.
9	1	196.11166	---	---	0.74E+00	9	2	195.25675	195.2565E (100)	-25	0.73E+00
9	2	196.20705	196.2073E (70)	24	0.75E+00	9	3	195.32940	195.3303E (70)	89	0.74E+00
9	3	196.37055	196.3713E (70)	75	0.24E+01	9	4	195.44747	195.4470E (70)	13	0.74E+00
9	4	196.59449	196.5952E (70)	28	0.81E+00	9	5	195.62008	195.6211E (70)	102	0.80E+00
9	5	196.89773	196.8976E (170)	-13	0.84E+00	9	6	195.83798	195.8370E (200)	-98	0.83E+00
9	6	197.26531	197.2644E (80)	-100	0.17E+01	9	7	196.0388	196.0360E (200)	211	0.17E+01
9	7	197.71858	197.7186E (50)	1	0.87E+00	9	8	196.41699	196.4170E (70)	6	0.85E+00
9	8	198.26042	198.2603E (70)	1	0.86E+00	9	9	196.77573	196.7756E (70)	6	0.78E+00
9	9	198.90101	198.9013E (70)	4	0.11E+01	10	0	214.10725	214.1115E (200)	21	0.11E+01
10	0	214.10841	---	---	0.	10	1	214.10705	---	---	0.73E+00
10	1	214.10841	214.1073E (80)	-94	0.37E+00	10	2	214.24810	214.2482E (80)	9	0.38E+00
10	2	214.01832	214.0193E (80)	78	0.38E+00	10	3	214.37920	214.3792E (80)	-9	0.38E+00
10	3	214.18216	214.1821E (80)	-96	0.79E+00	10	4	214.57058	---	---	0.41E+00
10	4	214.42613	214.4261E (200)	-1	0.44E+00	10	5	214.81368	214.8134E (80)	40	0.44E+00
10	5	214.73845	214.7380E (80)	-50	0.74E+00	10	6	215.02966	---	---	0.54E+00
10	6	216.12833	216.1291E (200)	58	0.95E+00	10	7	215.24906	215.2490E (80)	4	0.50E+00
10	7	216.40185	216.4020E (80)	14	0.50E+00	10	8	215.48045	215.4805E (80)	4	0.50E+00
10	8	217.18578	217.1857E (80)	-7	0.17E+01	10	9	215.80459	215.8045E (80)	80	0.51E+00
10	9	217.89052	217.8929E (70)	-97	0.97E+00	10	10	216.03093	216.0309E (80)	-13	0.50E+00
11	0	233.03381	233.0338E (70)	17	0.34E+00	11	1	216.02470	216.0257E (70)	100	0.35E+00
11	1	233.03381	233.0338E (60)	-17	0.10E+00	11	2	232.85821	---	---	0.
11	2	233.04304	233.0430E (60)	16	0.17E+00	11	3	232.88773	232.8878E (60)	6	0.16E+00
11	3	233.02745	233.0274E (60)	-5	0.36E+00	11	4	232.97845	232.9781E (60)	-34	0.17E+00
11	4	234.06932	234.0688E (200)	-56	0.19E+00	11	5	233.11455	233.1152E (60)	65	0.19E+00
11	5	234.39556	234.3953E (60)	24	0.21E+00	11	6	233.32748	---	---	0.19E+00
11	6	234.80102	234.8009E (60)	10	0.45E+00	11	7	233.59264	233.5926E (60)	25	0.20E+00
11	7	235.29261	235.2920E (200)	-61	0.28E+00	11	8	233.91786	233.9183E (60)	43	0.44E+00
11	8	235.87692	235.8767E (60)	-22	0.27E+00	11	9	234.36351	234.3633E (60)	-40	0.24E+00
11	9	236.50324	236.5030E (60)	-13	0.57E+00	11	10	234.74964	234.7496E (60)	-4	0.71E+00
12	0	251.36323	251.3630E (60)	-35	0.26E+00	12	1	235.25565	235.2556E (60)	-65	0.56E+00
12	1	251.36323	251.3632E (60)	-33	0.21E+00	12	2	235.61944	235.6190E (60)	-83	0.27E+00
12	2	251.96236	251.9622E (200)	-39	0.86E+01	12	3	236.03809	236.0379E (60)	-58	0.21E+00
12	3	252.07178	252.0715E (50)	-28	0.68E+01	12	4	251.37330	251.3730E (100)	59	0.13E+00
12	4	252.24390	252.2439E (100)	-200	0.14E+00	12	5	251.40475	251.4044E (100)	-34	0.66E+01
12	5	252.85142	252.8514E (100)	-5	0.77E+01	12	6	251.49917	251.4991E (80)	7	0.68E+01
12	6	253.05138	253.0513E (100)	-58	0.84E+01	12	7	251.60768	251.6067E (80)	-98	0.14E+00
12	7	253.27245	253.2725E (80)	5	0.19E+00	12	8	251.77947	251.7790E (100)	-46	0.77E+01
12	8	253.78061	---	---	0.11E+00	12	9	252.16455	252.1651E (80)	54	0.84E+01
12	9	254.38311	254.3830E (80)	-34	0.12E+00	12	10	252.31598	252.3159E (200)	-7	0.19E+00
12	10	254.88869	254.8886E (80)	91	0.27E+00	12	11	252.49366	252.4936E (80)	100	0.10E+00
12	11	255.08185	255.0820E (80)	-18	0.14E+00	12	12	253.09360	253.0936E (80)	96	0.12E+00
12	12	256.85683	256.8563E (50)	-11	0.15E+00	12	13	253.69992	---	---	0.26E+00
12	13	257.95307	257.9536E (50)	53	0.23E+00	12	14	254.29555	254.2955E (50)	56	0.14E+00
12	14	270.14232	270.1423E (100)	-1	0.47E+01	12	15	255.27155	255.2714E (50)	-34	0.14E+00
13	0	270.17992	270.1802E (80)	20	0.24E+01	12	16	256.03572	256.0362E (50)	47	0.22E+00
13	1	270.27300	270.2729E (100)	-39	0.25E+01	13	0	269.70760	269.7076E (50)	0	0.24E+01
13	2	270.48814	270.4882E (100)	186	0.52E+01	13	1	269.88819	269.8880E (80)	-136	0.24E+01
13	3	270.75370	270.7537E (100)	109	0.26E+01	13	2	269.96989	269.9696E (80)	391	0.22E+01
13	4	271.09955	271.0995E (60)	61	0.31E+01	13	3	270.12148	---	---	0.26E+00
13	5	271.53323	271.5332E (50)	6	0.60E+01	13	4	270.31768	---	---	0.31E+01
13	6	272.05842	272.0584E (80)	-263	0.40E+01	13	5	270.59580	270.5958E (80)	-10	0.40E+01
13	7</										

TABLE II
Inversion-Rotation Transition Wavenumbers (cm^{-1}) and Intensities ($\text{cm}^{-2} \text{atm}^{-1}$) of $^{14}\text{NH}_3$
in the ν_2 State^a

J	K	C	←←←		I	←←←		I
			O	(O-C)		O	(O-C)	
				$\times 10^3$			$\times 10^3$	
0	0	55.46537	—	—	0.	-15.55227	-15.55226 (1) ^b	0.246-03
1	0	74.74233	—	—	0.29E-01	—	—	—
1	1	75.12238	—	—	0.11E-01	4.67464	4.67468 (5)	4.42E-04
2	0	94.88753	—	—	0.	25.07478	25.07477 (1)	-1.04E-02
2	1	94.14034	—	—	0.24E-01	25.44601	25.44602 (1)	0.10E-02
2	2	94.00337	—	—	0.16E-01	24.74330	24.74330 (1)	0.11E-02
3	0	112.55355	112.55320(100)	35	0.74E-01	46.06899	—	—
3	1	112.77757	112.77700(100)	64	0.34E-01	46.06899	46.06899 (200)	9.0-06-02
3	2	113.59324	113.59310(100)	-38	0.30E-01	45.79994	45.80134 (300)	139.0-06-02
3	3	114.82141	114.82110(100)	-90	0.39E-01	44.65355	44.65340 (300)	-14.0-06-02
4	0	130.80351	—	—	0.	67.89529	67.89500 (80)	-29.0-02E-01
4	1	131.04679	131.04650(100)	-28	0.41E-01	67.68679	67.68750 (200)	71.0-11E-01
4	2	131.78190	131.78100(100)	-90	0.36E-01	67.05869	67.05810 (200)	-59.0-06E-02
4	3	133.03513	133.03480(100)	-37	0.45E-01	66.08267	66.08300 (100)	33.0-15E-01
4	4	134.86052	134.86100(100)	48	0.22E-01	64.41282	64.41250 (200)	-32.0-07E-02
5	0	146.73263	146.73160 (60)	-42	0.77E-01	89.23701	—	—
5	1	146.96788	146.96850(100)	61	0.30E-01	89.46829	89.46829 (80)	0.13E-01
5	2	149.67810	149.67800(100)	70	0.37E-01	88.42857	—	—
5	3	150.89078	150.89040 (80)	-37	0.69E-01	87.46045	—	—
5	4	152.65063	152.65020 (80)	-42	0.75E-01	85.95932	—	—
5	5	155.02644	155.02670 (300)	-174	0.20E-01	84.01354	—	—
6	0	166.39066	—	—	0.	110.44901	110.45130 (80)	138.0-07E-01
6	1	166.56738	166.56630 (100)	-107	0.31E-01	110.44872	—	—
6	2	167.24812	167.24780 (150)	-32	0.31E-01	109.93397	—	—
6	3	168.40255	168.40320 (100)	54	0.60E-01	109.01689	109.01690 (60)	1.0-02E-01
6	4	170.00446	170.00470 (100)	23	0.67E-01	107.67564	107.67610 (300)	46.0-11E-01
6	5	172.56945	172.56930 (90)	-14	0.25E-01	105.69064	105.69020 (40)	36.0-09E-02
6	6	175.32073	175.32060 (100)	-10	0.33E-01	103.45623	—	—
7	0	183.65759	183.65700 (200)	-58	0.43E-01	132.04731	—	—
7	1	183.87623	183.87600 (40)	21	0.25E-01	131.70031	—	—
7	2	184.92387	184.92370 (200)	-16	0.22E-01	131.41690	131.41520 (80)	-169.0-11E-01
7	3	185.62829	185.62830 (80)	0	0.44E-01	130.59260	130.59300 (100)	100.0-02E-01
7	4	187.22718	187.22760 (100)	-137	0.26E-01	129.37887	129.37810 (200)	-168.0-06E-01
7	5	189.38856	189.38800 (150)	-50	0.21E-01	127.71570	—	—
7	6	192.19130	192.19170 (60)	40	0.30E-01	125.53887	125.53970 (60)	83.0-10E-01
7	7	195.77461	195.77470 (60)	51	0.22E-01	122.77659	—	—
8	0	206.71832	—	—	0.	153.42260	—	—
8	1	206.96262	206.96260 (300)	-122	0.13E-01	153.26875	153.26930 (60)	-224.0-07E-02
8	2	201.94000	201.94110 (200)	109	0.14E-01	152.83009	152.83090 (80)	-59.0-07E-02
8	3	202.56286	202.56350 (100)	63	0.28E-01	152.10132	—	—
8	4	204.09863	204.09810 (100)	127	0.14E-01	151.01775	151.01870 (80)	95.0-07E-02
8	5	206.12468	206.12430 (60)	-34	0.36E-01	149.53500	—	—
8	6	208.76610	208.76540 (100)	-70	0.29E-01	147.56387	—	—
8	7	212.11514	212.11330 (100)	-183	0.13E-01	145.06582	—	—
8	8	216.30894	—	—	0.	143.44590	—	—
9	0	217.25598	217.25540 (250)	341	0.14E-01	174.05107	—	—
9	1	217.75732	—	—	0.73E-02	174.50911	—	—
9	2	217.93822	218.93170 (200)	—	0.16E-01	174.14826	—	—
9	3	219.30776	219.30300 (200)	-278	0.16E-01	173.30102	—	—
9	4	220.71236	—	—	0.61E-02	172.25999	172.53780 (100)	-319.0-09E-02
9	5	222.62903	222.62600 (110)	2	0.17E-01	171.25543	—	—
9	6	225.09107	225.09160 (100)	52	0.10E-01	169.51367	169.51340 (80)	-22.0-09E-02
9	7	228.22276	228.22370 (100)	94	0.02E-02	167.28301	—	—
9	8	232.14346	—	—	0.46E-02	166.42990	—	—
9	9	237.00027	237.00790 (100)	-36	0.13E-01	160.80068	—	—
10	0	234.20350	—	—	0.	195.69215	195.69070 (80)	-144.0-08E-02
10	1	234.97866	—	—	0.36E-02	195.59590	195.56180 (60)	250.0-08E-02
10	2	234.93571	—	—	0.37E-02	195.23997	—	—
10	3	235.80049	—	—	0.77E-02	194.68991	194.69080 (300)	88.0-05E-02
10	4	237.51646	—	—	0.41E-02	193.07332	—	—
10	5	238.91514	—	—	0.44E-02	192.74607	—	—
10	6	241.21106	—	—	0.93E-02	191.22601	—	—
10	7	244.11883	—	—	0.51E-02	189.31592	—	—
10	8	247.78699	—	—	0.24E-02	186.81713	—	—
10	9	252.27002	—	—	0.10E-01	183.62922	—	—
10	10	257.63663	—	—	0.39E-02	179.56670	—	—
11	0	250.40145	—	—	0.31E-02	216.49151	—	—
11	1	250.88149	—	—	0.16E-02	216.36197	—	—
11	2	251.36443	—	—	0.16E-02	216.09927	—	—
11	3	252.21799	—	—	0.36E-02	215.86937	—	—
11	4	253.40995	—	—	0.18E-02	214.92840	—	—
11	5	255.06851	—	—	0.20E-02	214.00424	—	—
11	6	257.11679	—	—	0.46E-02	212.73116	—	—
11	7	259.84992	—	—	0.24E-02	211.07817	—	—
11	8	263.20134	—	—	0.27E-02	208.92691	—	—
11	9	267.36033	—	—	0.50E-02	206.18549	—	—
11	10	272.50430	—	—	0.29E-02	202.66074	—	—
11	11	278.65978	—	—	0.23E-02	198.12648	—	—
12	0	267.04691	—	—	0.	237.00030	—	—
12	1	267.23781	—	—	0.62E-03	236.86273	—	—
12	2	267.71300	—	—	0.64E-03	236.66117	—	—
12	3	268.18444	—	—	0.14E-02	236.36280	—	—
12	4	269.54893	—	—	0.73E-03	235.74236	—	—
12	5	271.05379	—	—	0.00E-03	234.95481	—	—
12	6	271.90870	—	—	0.10E-02	233.90181	—	—
12	7	275.45760	—	—	0.10E-02	232.31861	—	—
12	8	278.52713	—	—	0.12E-02	230.71942	—	—
12	9	282.33806	—	—	0.27E-02	228.39544	—	—
12	10	287.05723	—	—	0.15E-02	225.36859	—	—
12	11	292.84699	—	—	0.13E-02	221.52037	—	—
12	12	300.62654	—	—	0.23E-02	216.54256	—	—
13	0	281.59315	—	—	0.44E-03	237.77908	—	—
13	1	283.49678	—	—	0.22E-03	236.99212	—	—
13	2	285.97493	—	—	0.26E-03	236.67943	—	—
13	3	289.42129	—	—	0.49E-03	236.05172	—	—
13	4	293.38397	—	—	0.20E-03	236.16173	—	—
13	5	298.59979	—	—	0.25E-03	235.25166	—	—
13	6	298.73532	—	—	0.66E-03	234.70822	—	—
13	7	299.97722	—	—	0.34E-03	233.57972	—	—
13	8	299.71251	—	—	0.44E-03	232.10915	—	—
13	9	297.13641	—	—	0.10E-02	230.10219	—	—
13	10	301.50933	—	—	0.61E-03	247.67930	—	—
13	11	304.70510	—	—	0.70E-03	244.42526	—	—
13	12	313.30218	—	—	0.15E-02	240.20299	—	—
13	13	321.36698	—	—	0.63E-03	234.78985	—	—

^a Our Fourier transform measurements unless stated otherwise (see Footnote^a in Table I).

^b Ref. (17); the $\alpha(0,0)$ energy level of the ν_2 state is higher than the $\alpha(1,0)$ level.

^c Ref. (10), ^d Ref. (1).

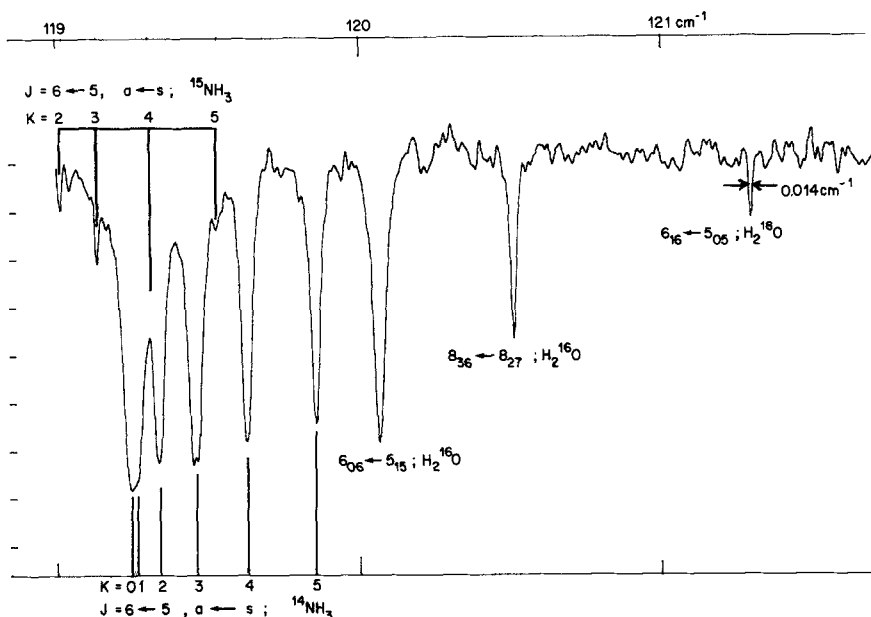


FIG. 1. Partly resolved K structure of the $s(5, K)$ multiplet of the ground-state inversion-rotation transitions of ammonia (apodized spectrum).

III. THEORETICAL MODEL AND THE SIMULTANEOUS ANALYSIS OF EXPERIMENTAL DATA

We have used the same fourth-order theory of the $\langle J, k | H | J, k \pm 3n \rangle$ interactions in the ground and ν_2 excited states of ammonia as described in the previous paper (2). We used the basis of the inversion-rotation wavefunctions

$$|^{(\pm)}\varphi_{i;J,k}\rangle = 2^{-1/2} \{ \psi_{i;J,k} \rangle [|J, k\rangle \pm |J, -k\rangle], \quad (1)$$

where the inversion wavefunctions $|\psi_{i;J,k}\rangle$ depend on the inversion coordinate ρ (as the dynamic variable) and on the rotational quantum numbers J and k as parameters.

In the basis of wavefunctions defined by Eq. (1), the secular problem for the ground and ν_2 state factorizes into two pairs of matrices for the *para*- NH_3 (E states) and four matrices for the *ortho*- NH_3 (A_1, A_2 states) [see Tables V and VI in Ref. (2)]. For reasons which we discussed in our previous paper (2), we used, for the diagonal matrix elements of the energy matrix, higher-order approximations compared to the fourth-order theory; in general these elements can be written as

$$\begin{aligned} {}^{(i)}E_0^{(m)}(J, K)/h = & {}^{(m)}E_0^{(m)}/h + B_m^{(i)}J(J+1) + (C_m^{(i)} - B_m^{(i)})K^2 - {}^{(i)}D_J^{(m)}J^2(J+1)^2 \\ & - {}^{(i)}D_{JK}^{(m)}J(J+1)K^2 - {}^{(i)}D_K^{(m)}K^4 + \sum_{n=0,1,2,3} {}^{(i)}H_{J_{3-n}K_n}^{(m)}[J(J+1)]^{3-n}K^{2n} \\ & + \sum_{n=0,1,2,3,4} {}^{(i)}G_{J_{4-n}K_n}^{(m)}[J(J+1)]^{4-n}K^{2n} + \sum_{n=0,1,2,3,4,5} {}^{(i)}L_{J_{5-n}K_n}^{(m)}[J(J+1)]^{5-n}K^{2n}. \quad (2) \end{aligned}$$

In Eq. (2), i indicates the parity of the state with respect to inversion [lower

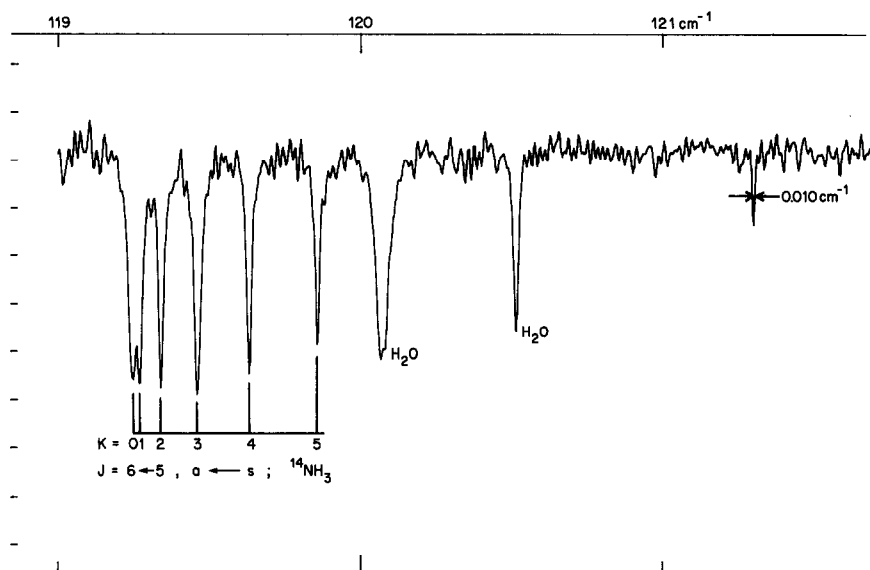


FIG. 2. Resolved K structure of the $s(5, K)$ multiplet of $^{14}\text{NH}_3$ (unapodized spectrum).

(denoted by s) or upper (denoted by a) component of the inversion doublet]; $m = 0$ for the ground state and $m = 1$ for the ν_2 state; a symbol like, for example, $^{(i)}G_{J_2K_2}^{(m)}$ means $^{(i)}G_{JJKK}^{(m)}$, etc.

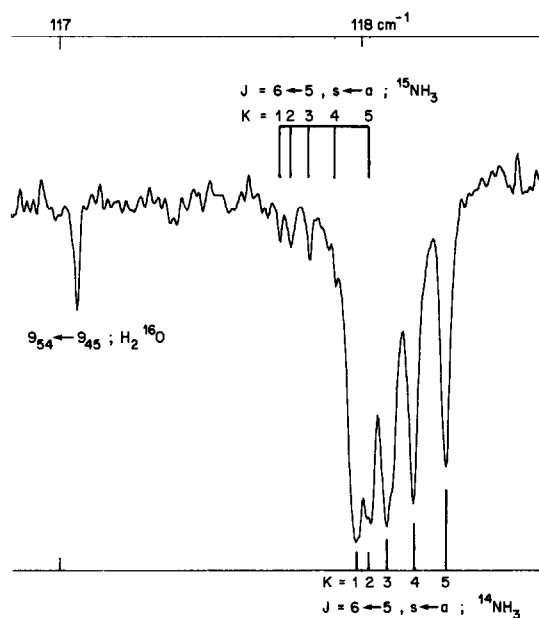


FIG. 3. Partly resolved K structure of the $a(5, K)$ multiplet of the ground-state inversion-rotation transitions of ammonia (apodized spectrum).

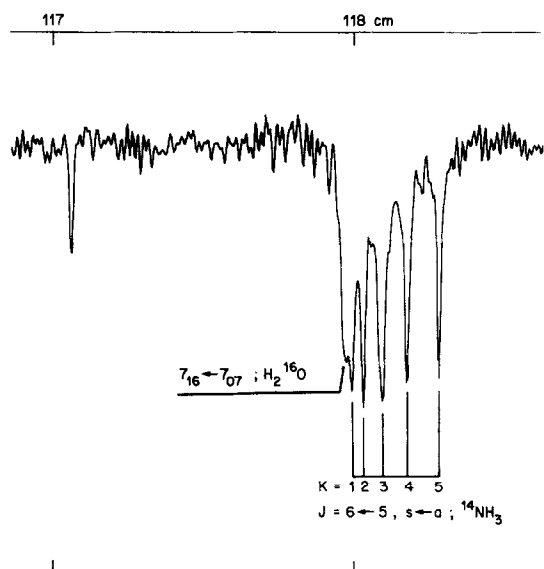


FIG. 4. Resolved K structure of the $a(5, K)$ multiplet of the ground-state inversion-rotation transitions of $^{14}\text{NH}_3$ (unapodized spectrum).

The operators which describe the $\Delta k = \pm 3n$ interactions in the ground state and ν_2 excited state are defined as follows:

$$H'_1 = H_2(\rho)[(J_+^3 + J_-^3)J_z + J_z(J_+^3 + J_-^3)], \quad (3a)$$

$$H'_2 = H_3(\rho)(J_+^3 - J_-^3), \quad (3b)$$

$$H'_3 = [H_1(\rho) + H_4(\rho) + H_5(\rho)](J_+^6 + J_-^6), \quad (3c)$$

$$H'_4 = H(\rho)(J_+^{12} + J_-^{12}), \quad (3d)$$

where the operators $H_1(\rho)$ – $H_5(\rho)$ have been explicitly defined in our previous paper (2) and $J_{\pm} = J_x \pm iJ_y$. Note that the $H_3(\rho)$ operator is antisymmetric in the basis of the inversion wavefunctions and thus H'_2 is Hermitian (2); H'_2 is invariant with respect to the time reversal [cf. definition of $H_3(\rho)$ in Ref. (2)]. The operator H'_4 is beyond the approximation in which the theory of the $\Delta k = \pm 3n$ interactions was discussed in Ref. (2); we have found by the numerical analysis of the experimental data that the matrix element of this operator diagonal in K should be introduced.

There are the following matrix elements of the operators in Eq. (3) in the basis of wavefunctions $|\varphi_{(a)}^{(s)}; J, k\rangle = |\psi_{(a)}^{(s)}; J, k\rangle \cdot |J, k\rangle$:

$$\begin{aligned} \langle \varphi_{(a)}^{(s)}; J, k | H'_1 | \varphi_{(a)}^{(s)}; J, k \rangle &= \hbar^4 \langle \psi_{(a)}^{(s)}; J, k | H_2(\rho) | \psi_{(a)}^{(s)}; J, k \rangle \\ &\times (2k \pm 3) \prod_{i=0}^{i=2} [J(J+1) - (k \pm i)(k \pm i \pm 1)]^{1/2}, \quad (4) \end{aligned}$$

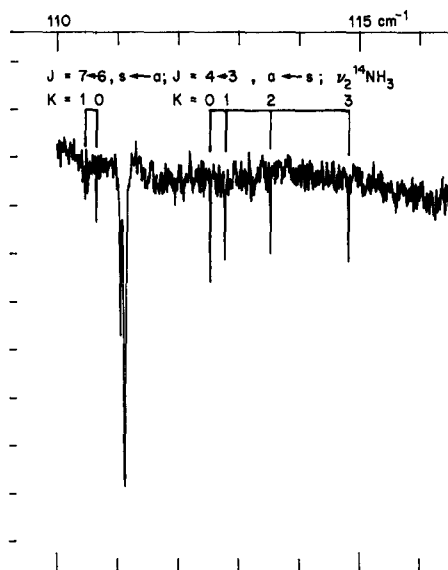


FIG. 5. Resolved K structure of the $s(3, K)$ multiplet of the inversion-rotation transitions in the ν_2 excited state of $^{14}\text{NH}_3$ (apodized spectrum).

$$\langle \varphi_{(a)}^{(s);J,k} | H'_2 | \varphi_{(a)}^{(s);J,k\pm 3} \rangle = \pm \hbar^3 \langle \psi_{(a)}^{(s);J,k} | H_3(\rho) | \psi_{(a)}^{(s);J,k\pm 3} \rangle \times \prod_{i=0}^{i=2} [J(J+1) - (k \pm i)(k \pm i \pm 1)]^{1/2}. \quad (5)$$

From the matrix elements of the operators H'_3 and H'_4 [Eqs. (3c) and (3d)], we have considered only those which contribute to the main diagonal of the interaction matrix:

$$\langle \varphi_{(a)}^{(s);J,-3} | H'_3 | \varphi_{(a)}^{(s);J,+3} \rangle = \hbar^6 \langle \psi_{(a)}^{(s);J,-3} | H_1(\rho) + H_4(\rho) + H_5(\rho) | \psi_{(a)}^{(s);J,+3} \rangle [(J+3)/(J-3)!], \quad (6)$$

$$\langle \varphi_{(a)}^{(s);J,-6} | H'_4 | \varphi_{(a)}^{(s);J,+6} \rangle = \hbar^{12} \langle \psi_{(a)}^{(s);J,-6} | H(\rho) | \psi_{(a)}^{(s);J,+6} \rangle \times [(J+6)/(J-6)!]. \quad (7)$$

Let us denote

$$h^{-3}c(2\pi)^4\alpha = \langle \psi_{(a)}^{(s);J,k} | H_2(\rho) | \psi_{(a)}^{(s);J,k\pm 3} \rangle = \langle \psi_{(a)}^{(s);J,k\pm 3} | H_2(\rho) | \psi_{(a)}^{(s);J,k} \rangle, \quad (8)$$

$$h^{-2}c(2\pi)^3\beta = -\langle \psi_{(a)}^{(s);J,k} | H_3(\rho) | \psi_{(a)}^{(s);J,k\pm 3} \rangle = +\langle \psi_{(a)}^{(s);J,k\pm 3} | H_3(\rho) | \psi_{(a)}^{(s);J,k} \rangle, \quad (9)$$

$$h^{-5}c(2\pi)^6\eta_3^{(s)} = \langle \psi_{(a)}^{(s);J,-3} | H_1(\rho) + H_4(\rho) + H_5(\rho) | \psi_{(a)}^{(s);J,3} \rangle, \quad (10)$$

$$h^{-11}c(2\pi)^{12}\eta_6^{(s)} = \langle \psi_{(a)}^{(s);J,-6} | H(\rho) | \psi_{(a)}^{(s);J,6} \rangle, \quad (11)$$

where α , β , and η are in cm^{-1} .

We have found that the experimental data used in the present paper do not allow for a separate determination of $\eta_t^{(s)}$ and $\eta_t^{(a)}$ ($t = 3, 6$); only $\eta_t = (\eta_t^{(s)} + \eta_t^{(a)})/2$ can be determined. On the other hand, we found that the dependence of η_t on the rotational quantum numbers should be taken into account because of the

TABLE III

Inversion Transition Wavenumbers (cm^{-1}) and Intensities ($\text{cm}^{-2} \text{atm}^{-1}$) of $^{14}\text{NH}_3$ in the ν_2 State^a

J	K	C	O	(O-C)	I	J	K	C	O	(O-C)	I
				$\times 10^5$						$\times 10^5$	
3	0	35.888111	-----	-----	0.	9	8	35.55552	35.55554(1)	31	1 0.12E-02
1	0	35.324941	-----	-----	0.	9	9	35.49987	-----	-----	0.50E-02
1	3	35.57564	35.57564(1)	0	0.27E-02	10	0	20.34877	-----	-----	0.
2	0	34.622681	-----	-----	0.	10	1	20.51572	20.51570(1)	101	-1 0.76E-06
2	1	34.86101	34.86081(3)	-1	0.12E-02	10	2	20.46742	20.46739(1)	5)	-3 0.33E-05
2	2	35.61387	35.61386(1)	0	0.53E-02	10	3	21.74793	21.74790(1)	5)	5 0.17E-04
3	0	33.55004	-----	-----	0.	10	4	22.85480	-----	-----	0.19E-04
3	1	33.82624	33.82620(1)	-3	0.59E-03	10	5	24.38304	-----	-----	0.40E-04
3	2	34.55112	34.55111(3)	-1	0.26E-03	10	6	26.37895	26.37886(1)	3)	1 0.16E-03
3	3	33.79306	33.79312(1)	5)	0.14E-01	10	7	28.93145	28.93146(1)	6)	1 0.16E-03
4	0	32.25252	-----	-----	0.	10	8	32.15759	32.15759(1)	5)	0 0.34E-03
4	1	32.49538	32.49536(1)	-2	0.29E-03	10	9	36.10832	36.10835(167)	22	0.14E-02
4	2	33.18123	33.18121(1)	-1	0.23E-02	10	10	41.27756	-----	-----	0.16E-02
4	3	34.37480	34.37482(1)	2)	0.67E-02	11	0	18.16258	-----	-----	0.
4	4	36.11141	36.11105(167)	23	0.74E-02	11	1	18.32285	-----	-----	0.20E-06
5	0	30.65570	-----	-----	0.	11	2	18.72032	18.72022(1)	5)	-9 0.88E-06
5	1	30.87663	30.87661(1)	-2	0.13E-03	11	3	19.36264	19.36260(1)	5)	4 0.46E-05
5	2	31.54108	31.54108(1)	0	0.59E-03	11	4	20.32337	20.32335(1)	5)	-1 0.51E-05
5	3	32.67766	32.67761(1)	-5)	0.31E-02	11	5	21.78603	21.78600(1)	5)	-2 0.10E-04
5	4	34.33628	34.33624(1)	-4	0.34E-02	11	6	23.57961	23.57961(1)	6)	0 0.42E-04
5	5	36.57523	36.57507(100)	3)	0.71E-02	11	7	25.87546	25.87548(1)	5)	2 0.43E-04
6	0	28.83928	-----	-----	0.	11	8	28.78027	28.78027(1)	6)	0 0.80E-04
6	1	29.49434	-----	-----	0.27E-04	11	9	32.43248	32.43249(1)	3)	0 0.38E-03
6	2	29.67725	29.67750(1)	2)	0.23E-03	11	10	37.01038	37.01127(134)	88	0.42E-03
6	3	30.75267	30.75262(1)	-5)	0.13E-02	11	11	42.74215	-----	-----	0.97E-03
6	4	32.31602	32.31602(1)	0	0.15E-02	12	0	16.03772	-----	-----	0.
6	5	34.43457	34.43459(1)	2)	0.30E-02	12	1	16.15667	-----	-----	0.40E-07
6	6	37.19513	-----	-----	0.82E-01	12	2	16.55685	-----	-----	0.21E-06
7	0	26.85067	-----	-----	0.	12	3	17.15097	-----	-----	0.11E-05
7	1	27.04521	27.04521(1)	0	0.22E-04	12	4	18.03823	18.03833(1)	5)	0 0.12E-05
7	2	27.63860	27.63852(1)	-8	0.09E-04	12	5	19.25823	-----	-----	0.29E-05
7	3	28.63299	28.63295(1)	-4	0.32E-03	12	6	20.85313	20.85310(1)	5)	-1 0.10E-04
7	4	30.10260	30.10260(1)	0	0.37E-03	12	7	22.85628	22.85630(1)	5)	2 0.10E-04
7	5	32.08504	32.08504(1)	0	0.12E-02	12	8	25.48916	25.48917(1)	3)	0 0.21E-04
7	6	34.68935	34.68934(1)	1	0.48E-02	12	9	28.74235	28.74231(1)	6)	-4 0.90E-04
7	7	37.96868	-----	-----	0.49E-02	12	10	32.83318	32.83271(134)	-46	0.10E-03
8	0	24.73559	-----	-----	0.	12	11	37.96518	-----	-----	0.23E-03
8	1	24.92879	24.92880(1)	1	0.80E-05	12	12	44.40482	-----	-----	0.11E-02
8	2	25.47037	25.47040(1)	3)	0.15E-04	13	0	14.00889	-----	-----	0.
8	3	26.40270	26.40265(1)	-5)	0.18E-03	13	1	14.17841	-----	-----	0.10E-07
8	4	27.75151	27.75151(1)	0	0.20E-03	13	2	14.45498	-----	-----	0.44E-07
8	5	29.58776	29.58776(1)	0	0.42E-03	13	3	14.85186	-----	-----	0.24E-06
8	6	31.98108	31.98106(1)	-2	0.17E-02	13	4	15.57996	-----	-----	0.26E-06
8	7	35.04162	35.04163(1)	0	0.17E-02	13	5	16.84076	-----	-----	0.34E-06
8	8	38.89613	-----	-----	0.36E-02	13	6	18.24387	18.24381(1)	5)	-5 0.22E-05
9	0	22.55614	-----	-----	0.	13	7	20.04271	20.04271(1)	5)	0 0.22E-05
9	1	22.73248	22.73248(1)	0	0.26E-05	13	8	22.32595	22.32595(1)	5)	3 0.42E-05
9	2	23.23054	23.23055(1)	1	0.11E-04	13	9	25.15906	25.15902(1)	3)	-3 0.19E-04
9	3	24.05884	24.05877(1)	-7	0.60E-04	13	10	28.81548	28.81527(167)	-20	0.21E-04
9	4	25.31757	25.31755(1)	-2	0.66E-04	13	11	33.36146	33.36147(1)	7)	1 0.40E-04
9	5	27.00140	27.00141(1)	0	0.14E-03	13	12	39.07915	-----	-----	0.24E-03
9	6	29.15925	29.15916(1)	0	0.35E-03	13	13	46.27802	-----	-----	0.30E-03
9	7	32.00770	32.00778(1)	7)	0.56E-03						

^a Our submillimeterwave measurements of the $\Delta J = 0$, $\Delta K = 0$ transitions with the spectrometer RAD [see also Refs. (1, 2)]; cf. footnote a of Table I for the labeling of columns and meaning of parentheses in the calculated and observed wavenumbers. In measurements where transition wavenumbers were determined by interpolating between the calibration lines, the experimental uncertainties are higher than 10^{-4} cm^{-1} [cf. Ref. (2)].

parametric dependence of η_i on the rotational quantum numbers J, K . A simple perturbation treatment shows that the J, K dependence of η_i must have the form

$$\eta_3 = \eta_3^0 + \eta_3^J J(J+1) + \eta_3^K K^2 + \eta_3^{JJ} J^2(J+1)^2 + \eta_3^{KK} K^4 + \eta_3^{JK} J(J+1)K^2 + \text{higher-order terms} \quad (12)$$

and

$$\eta_6 = \eta_6^0 + \eta_6^J J(J+1) + \eta_6^K K^2 + \text{higher-order terms}. \quad (13)$$

The numerical treatment of our problem was based on the following procedure: (i) Using a second-order perturbation theory, we have diagonalized the interaction matrices for the *ortho*- and *para*- states of ammonia to obtain analytical expressions for the energy levels E_k as functions of the molecular parameters Φ_k ($k = 1, 2, \dots, r$):

$$E_j = f_j(\Phi_1, \Phi_2, \dots, \Phi_r). \quad (14)$$

(ii) From these expressions, analytical expressions have been obtained for the elements of the Jacobian matrix

$$\partial E_j / \partial \Phi_k = J_{j,k}^{(E)}(\Phi_1, \Phi_2, \dots, \Phi_r). \quad (15)$$

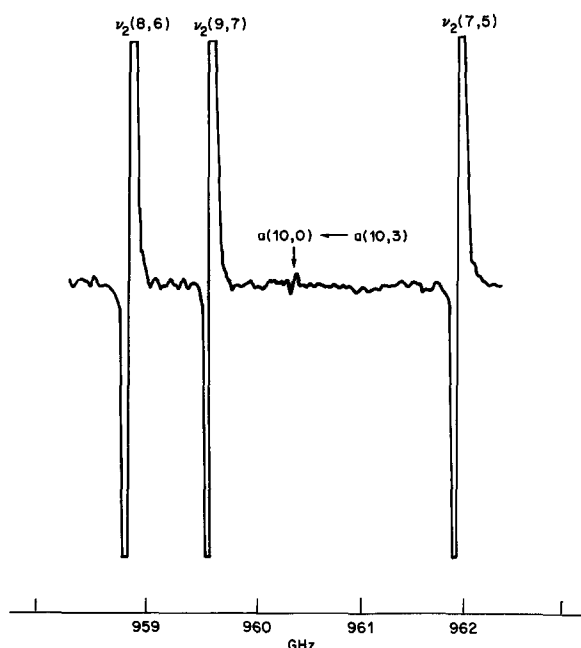


FIG. 6. Part of the submillimeterwave spectrum of ammonia at 960 GHz illustrating the sensitivity of the spectrometer RAD (see the calculated intensities of the spectrum lines in Tables II and V). $\nu_2(J, K)$ denote the lines of the $a(J, K) \leftarrow s(J, K)$ inversion transitions in the ν_2 excited state; $a(10, 0) \leftarrow a(10, 3)$ denotes the line of the ground-state perturbation-allowed transition.

(iii) For a given frequency ν_{pq} of the transition between the energy levels E_p and E_q , the Jacobian matrix was obtained simply as

$$\partial \nu_{pq} / \partial \Phi_k (J_{p,k}^{(E)} - J_{q,k}^{(E)}) / h. \quad (16)$$

(iv) The minimum of the function

$$F(\Phi) = \sum_{p,q} w_{pq} [\nu_{pq}^{(\text{calc})} - \nu_{pq}^{(\text{exp})}]^2 \quad (17)$$

has been found by using the method of damped least-squares (19). In Eq. (17), summation extends over all the experimental data; w_{pq} are their statistical weights.

It is convenient to introduce the following vectors of molecular parameters which can, in principle, be determined from the experimental data used in our work:

$$X_m^{(J)} = B_m^{(s)}, {}^{(s)}D_J^{(m)}, {}^{(s)}H_{JJJ}^{(m)}, \dots, {}^{(s)}L_{JJJJJ}^{(m)}, \quad (18)$$

$$X_m^{(JK)} = {}^{(s)}D_{JK}^{(m)}, {}^{(s)}H_{JJK}^{(m)}, {}^{(s)}H_{JKK}^{(m)}, \dots, {}^{(s)}L_{JKKKK}^{(m)}, \quad (19)$$

$$X_m^{(K)} = C_m^{(s)} - B_m^{(s)}, {}^{(s)}D_K^{(m)}, {}^{(s)}H_{KKK}^{(m)}, \dots, {}^{(s)}L_{KKKKK}^{(m)}, \quad (20)$$

$$\Delta X_m = \Delta E_m, \Delta B_m, \Delta(C_m - B_m), \Delta D_J^{(m)}, \Delta D_{JK}^{(m)}, \Delta D_K^{(m)}, \Delta H_{JJJ}^{(m)}, \dots, \Delta L_{KKKKK}^{(m)}; \quad (21)$$

in the last equation, the general term $\Delta X_j^{(m)}$ is defined as

$$\Delta X_j^{(m)} = {}^{(a)}X_j^{(m)} - {}^{(s)}X_j^{(m)}, \quad (22)$$

where ${}^{(i)}X_j^{(m)}$ stands for any one of the elements on the right-hand side of Eq. (21).

TABLE IV

Transition Wavenumbers (cm^{-1}) and Intensities ($\text{cm}^{-2} \text{atm}^{-1}$) in the ν_2 Band of $^{14}\text{NH}_3^a$

J	K	C	aP(J,K)		I	C	aP(J,K)		I
			0	(0-C)			0	(0-C)	
				$\times 10^3$				$\times 10^3$	
1	0	911.76058	—	0.	0.	948.23206	948.23200(200) ^b	74	0.28E+01
2	0	892.15606	—	0.45E+01	(928.24988)	—	—	—	0.
2	1	891.40192	—	0.17E+01	928.23205	—	—	—	0.17E+01
3	0	872.04138	—	0.	906.19918	—	—	—	0.30E+01
3	1	872.56713	—	0.23E+01	906.17691	—	—	—	0.23E+01
3	2	871.73682	—	0.13E+01	906.11235	—	—	—	0.13E+01
4	0	853.01792	—	0.45E+01	(888.10672)	—	—	—	0.
4	1	853.54827	—	0.21E+01	888.07968	888.07790(30)E	-157	0.21E+01	0.15E+01
4	2	852.72481	—	0.18E+01	887.99987	887.99900(30)E	-107	0.18E+01	0.10E+01
4	3	851.32699	—	0.23E+01	887.82883	887.82603(30)E	-1	0.23E+01	0.15E+01
5	0	833.09327	—	0.	866.90370	—	—	—	0.34E+01
5	1	834.02392	—	0.17E+01	867.96981	—	—	—	0.16E+01
5	2	834.01228	—	0.15E+01	867.87302	—	—	—	0.15E+01
5	3	832.03498	—	0.25E+01	867.71368	—	—	—	0.25E+01
5	4	830.65313	—	0.40E+00	867.52817	—	—	—	0.40E+00
6	0	816.65317	—	0.22E+01	(847.91496)	—	—	—	0.
6	1	816.38644	—	0.11E+01	847.87034	—	—	—	0.11E+01
6	2	815.59122	—	0.11E+01	847.76313	—	—	—	0.11E+01
6	3	814.24150	—	0.20E+01	847.57829	—	—	—	0.20E+01
6	4	812.30117	—	0.02E+00	847.33772	—	—	—	0.02E+00
6	5	809.71476	—	0.53E+00	847.09137	—	—	—	0.53E+00
7	0	798.48201	—	0.	827.87012	—	—	—	0.18E+01
7	1	798.22265	—	0.06E+00	827.83375	—	—	—	0.06E+00
7	2	797.44604	—	0.25E+00	827.78227	—	—	—	0.06E+00
7	3	796.13435	—	0.13E+01	827.48801	—	—	—	0.12E+01
7	4	794.24416	—	0.50E+00	827.20225	—	—	—	0.50E+00
7	5	791.72882	—	0.50E+00	826.95327	—	—	—	0.50E+00
7	6	788.51039	—	0.65E+00	826.47021	—	—	—	0.65E+00
8	0	780.56828	—	0.09E+00	(807.82283)	—	—	—	0.
8	1	780.31481	—	0.35E+00	807.87225	—	—	—	0.34E+00
8	2	779.56494	—	0.35E+00	807.72283	—	—	—	0.34E+00
8	3	778.29030	—	0.09E+00	807.47225	—	—	—	0.09E+00
8	4	776.60186	—	0.34E+00	807.14433	—	—	—	0.34E+00
8	5	774.02335	—	0.32E+00	806.73761	—	—	—	0.32E+00
8	6	770.01381	—	0.50E+00	806.27428	—	—	—	0.50E+00
8	7	767.03743	—	0.19E+00	805.77988	—	—	—	0.19E+00
9	0	762.88910	—	0.	788.82408	—	—	—	0.10E+00
9	1	762.64169	—	0.16E+00	788.80249	—	—	—	0.16E+00
9	2	761.91909	—	0.17E+00	787.95534	—	—	—	0.16E+00
9	3	760.67682	—	0.34E+00	787.77689	—	—	—	0.34E+00
9	4	758.93089	—	0.17E+00	787.19941	—	—	—	0.17E+00
9	5	756.58442	—	0.17E+00	786.73250	—	—	—	0.17E+00
9	6	753.29053	—	0.33E+00	786.39067	—	—	—	0.33E+00
9	7	749.86304	—	0.13E+00	785.99632	—	—	—	0.13E+00
9	8	745.29234	—	0.10E+00	784.98060	—	—	—	0.10E+00
10	0	745.42118	—	0.14E+00	(768.37488)	—	—	—	0.
10	1	745.17958	—	0.09E+01	768.31292	—	—	—	0.08E+01
10	2	744.48759	—	0.71E+01	768.12964	—	—	—	0.70E+01
10	3	743.30766	—	0.15E+00	767.91082	—	—	—	0.14E+00
10	4	741.62224	—	0.76E+01	767.89693	—	—	—	0.75E+01
10	5	739.37522	—	0.79E+01	766.87308	—	—	—	0.78E+01
10	6	736.50924	—	0.16E+00	766.23274	—	—	—	0.16E+00
10	7	732.94356	—	0.80E+01	765.96119	—	—	—	0.79E+01
10	8	728.37447	—	0.73E+01	764.82355	—	—	—	0.74E+01
10	9	723.87000	—	0.10E+00	764.07767	—	—	—	0.10E+00
11	0	728.14114	—	0.	748.87821	—	—	—	0.22E+01
11	1	727.90389	—	0.27E+01	748.76924	—	—	—	0.26E+01
11	2	727.24537	—	0.27E+01	748.57171	—	—	—	0.27E+01
11	3	726.12588	—	0.17E+01	748.22825	—	—	—	0.16E+01
11	4	724.51070	—	0.30E+01	747.76402	—	—	—	0.29E+01
11	5	722.36802	—	0.32E+01	747.18213	—	—	—	0.31E+01
11	6	719.63736	—	0.08E+01	746.49063	—	—	—	0.07E+01
11	7	716.24294	—	0.36E+01	745.70586	—	—	—	0.35E+01
11	8	712.08748	—	0.36E+01	744.93089	—	—	—	0.36E+01
11	9	707.09107	—	0.08E+01	743.68023	—	—	—	0.09E+01
11	10	706.06590	—	0.25E+01	743.07345	—	—	—	0.25E+01
12	0	711.02489	—	0.10E+01	(729.46011)	—	—	—	0.
12	1	710.78987	—	0.42E+02	729.44602	—	—	—	0.41E+02
12	2	710.16804	—	0.95E+02	729.20584	—	—	—	0.93E+02
12	3	709.09072	—	0.20E+01	728.81481	—	—	—	0.20E+01
12	4	707.56181	—	0.11E+01	728.32490	—	—	—	0.10E+01
12	5	705.53314	—	0.11E+01	727.69032	—	—	—	0.11E+01
12	6	702.94223	—	0.25E+01	726.93850	—	—	—	0.25E+01
12	7	699.72517	—	0.14E+01	726.09826	—	—	—	0.14E+01
12	8	695.79110	—	0.15E+01	725.09283	—	—	—	0.15E+01
12	9	691.02433	—	0.31E+01	724.06144	—	—	—	0.31E+01
12	10	685.27900	—	0.15E+01	723.00282	—	—	—	0.15E+01
12	11	678.37215	—	0.11E+01	721.97141	—	—	—	0.11E+01
13	0	694.05094	—	0.	710.34300	—	—	—	0.50E+02
13	1	693.01340	—	0.29E+02	710.26660	—	—	—	0.29E+02
13	2	693.23313	—	0.30E+02	710.05330	—	—	—	0.29E+02
13	3	692.23520	—	0.03E+02	709.64282	—	—	—	0.02E+02
13	4	690.76912	—	0.34E+02	709.07970	—	—	—	0.33E+02
13	5	688.84278	—	0.37E+02	708.43710	—	—	—	0.36E+02
13	6	686.39323	—	0.02E+02	707.59415	—	—	—	0.01E+02
13	7	683.25589	—	0.06E+02	706.65845	—	—	—	0.05E+02
13	8	679.64656	—	0.31E+02	705.57931	—	—	—	0.31E+02
13	9	675.15625	—	0.11E+01	704.43472	—	—	—	0.11E+01
13	10	669.75516	—	0.02E+02	703.19468	—	—	—	0.02E+02
13	11	663.26701	—	0.01E+02	701.95998	—	—	—	0.02E+02
13	12	655.48143	—	0.95E+02	700.77537	—	—	—	0.94E+02
14	0	677.20898	—	0.17E+02	(691.42371)	—	—	—	0.
14	1	676.98463	—	0.16E+03	691.38360	—	—	—	0.16E+03
14	2	676.42147	—	0.07E+03	691.18784	—	—	—	0.06E+03
14	3	675.44469	—	0.10E+02	690.05913	—	—	—	0.10E+02
14	4	674.09142	—	0.09E+02	690.10827	—	—	—	0.09E+02
14	5	672.27231	—	0.11E+02	689.87890	—	—	—	0.11E+02
14	6	669.98273	—	0.74E+02	688.49982	—	—	—	0.74E+02
14	7	667.10165	—	0.14E+02	687.71777	—	—	—	0.14E+02
14	8	663.61837	—	0.10E+02	686.31473	—	—	—	0.10E+02
14	9	659.40817	—	0.17E+02	685.03924	—	—	—	0.16E+02
14	10	654.34792	—	0.11E+02	683.97273	—	—	—	0.11E+02
14	11	648.28023	—	0.23E+02	682.25237	—	—	—	0.24E+02
14	12	641.00783	—	0.48E+02	680.83261	—	—	—	0.49E+02
14	13	632.28507	—	0.19E+02	679.48849	—	—	—	0.20E+02

^a C and D are calculated and observed transition wavenumbers, I are calculated intensities. Values in parentheses of the observed wavenumbers are estimated experimental uncertainties in units of the last digit quoted; $\alpha(J,K)$ and $\alpha(J,K)$ with $X = P, Q, R$ denote transitions from the lower (s) or upper (u) component of the ground state inversion doublets. Calculated wavenumbers for transitions from levels with zero spin statistical weights are in parentheses. ^b Ref. (24). ^c Ref. (8). ^d Ref. (9). ^e Ref. (7). ^f Ref. (25). ^g Ref. (1).

TABLE IV—Continued

$\omega(J, K)$						$\omega(J, K)$						
J	K	C	D	(O-C)	I	J	K	C	D	(O-C)	I	
$\times 10^5$						$\times 10^5$						
0	0	0	931.04043	—	—	0	0	0	968.12195	—	0.	
1	0	1	931.05621	—	—	1	0	1	968.08912	—	0.	
1	1	0	931.02778	931.02776 (20) ^a	-1	1	0	0	967.99778	967.99774 (10) ^a	-3	0.22E+01
2	0	0	931.04013	—	—	2	0	0	967.77768	—	—	0.
2	1	0	931.13619	932.13618 (20) ^a	-9	2	0	1	967.77779	—	—	0.10E+01
2	2	0	931.33328	931.33324 (20) ^a	14	2	0	0	967.73894	967.73894 (10) ^a	14	0.92E+01
3	0	0	931.13884	—	—	3	0	0	967.64480	—	—	0.
3	1	0	931.00129	—	—	3	0	1	967.44926	—	—	0.53E+00
3	2	0	932.09408	932.09402 (20) ^a	-5	3	0	0	967.40888	—	—	0.22E+01
3	3	0	930.75706	—	—	3	0	1	967.34634	967.34632 (20) ^a	-1	0.11E+02
4	0	0	931.00017	—	—	4	0	0	967.04824	—	—	0.
4	1	0	931.04256	933.04190 (50) ^c	-66	4	0	0	967.03891	—	—	0.29E+00
4	2	0	931.07957	933.07620 (100) ^b	33	4	0	1	966.98104	—	—	0.12E+01
4	3	0	931.77394	—	—	4	0	1	966.90520	—	—	0.50E+01
4	4	0	929.89813	929.89820 (50) ^c	6	4	0	0	966.81479	—	—	0.59E+01
5	0	0	931.26108	—	—	5	0	0	966.52269	—	—	0.
5	1	0	931.09048	—	—	5	0	0	966.53244	—	—	0.14E+00
5	2	0	931.25220	934.25240 (50) ^c	20	5	0	0	966.47370	—	—	0.59E+00
5	3	0	932.99235	932.99243 (15) ^a	8	5	0	0	966.38001	—	—	0.29E+01
5	4	0	931.17737	931.17731 (30) ^a	-2	5	0	1	966.28928	966.28931 (10) ^a	2	0.29E+01
5	5	0	929.75649	929.75620 (50) ^c	-19	5	0	1	966.15116	966.15100 (10) ^a	-15	0.
6	0	0	931.94301	—	—	6	0	0	965.94128	—	—	0.
6	1	0	931.30498	—	—	6	0	0	965.90779	—	—	0.47E+01
6	2	0	931.59177	—	—	6	0	0	965.89924	—	—	0.28E+00
6	3	0	931.37669	—	—	6	0	1	965.79140	—	—	0.14E+01
6	4	0	932.63573	932.63589 (10) ^c	15	6	0	1	965.65206	—	—	0.14E+01
6	5	0	930.30645	930.30631 (20) ^a	-1	6	0	1	965.49948	—	—	0.24E+01
6	6	0	927.32303	927.32328 (10) ^c	24	6	0	0	965.35393	—	—	0.90E+01
7	0	0	937.77028	—	—	7	0	0	965.37870	—	—	0.
7	1	0	937.74072	—	—	7	0	0	965.35178	—	—	0.90E+01
7	2	0	937.05956	—	—	7	0	0	965.27294	—	—	0.13E+00
7	3	0	935.90392	—	—	7	0	0	965.11790	965.11730 (100) ^a	-59	0.62E+00
7	4	0	934.23583	934.23580 (50) ^c	-2	7	0	0	964.97769	—	—	0.63E+00
7	5	0	932.01123	—	—	7	0	0	964.79825	964.79806 (10) ^a	-18	0.11E+01
7	6	0	929.16174	929.16160 (30) ^c	-13	7	0	0	964.59579	964.59540 (100) ^a	-38	0.40E+01
7	7	0	925.59908	—	—	7	0	0	964.42485	964.42410 (20) ^a	5	0.94E+01
8	0	0	930.44628	—	—	8	0	0	964.72059	—	—	0.
8	1	0	930.20424	—	—	8	0	0	964.69915	—	—	0.12E+01
8	2	0	930.42804	—	—	8	0	0	964.53501	—	—	0.52E+01
8	3	0	937.51597	—	—	8	0	0	964.46735	—	—	0.29E+00
8	4	0	935.93753	—	—	8	0	0	964.24870	—	—	0.24E+00
8	5	0	933.62674	933.62660 (40) ^a	-13	8	0	0	964.06118	—	—	0.47E+00
8	6	0	931.12203	931.12190 (20) ^a	-13	8	0	0	963.79623	—	—	0.10E+01
8	7	0	927.74201	927.74196 (30) ^a	-5	8	0	0	963.59588	963.59520 (100) ^a	-68	0.14E+01
9	0	0	941.05128	—	—	9	0	0	963.36278	963.36262 (10) ^a	-16	0.24E+01
9	1	0	940.89718	—	—	9	0	0	964.02322	—	—	0.
9	2	0	940.22849	—	—	9	0	0	963.97511	—	—	0.47E+02
9	3	0	935.19865	—	—	9	0	0	963.71705	—	—	0.59E+01
9	4	0	937.69933	937.69890 (50) ^c	-43	9	0	0	963.51473	—	—	0.98E+01
9	5	0	935.70766	—	—	9	0	0	963.26939	—	—	0.18E+00
9	6	0	931.15746	933.15710 (100) ^a	-37	9	0	0	962.97370	962.97368 (20) ^a	-1	0.63E+00
9	7	0	929.07044	929.07110 (50) ^a	61	9	0	0	962.64984	—	—	0.54E+00
9	8	0	926.06576	926.06584 (20) ^a	7	9	0	0	962.38842	—	—	0.91E+00
9	9	0	921.25508	—	—	9	0	0	962.17131	—	—	0.31E+01
10	0	0	942.62850	—	—	10	0	0	963.37472	—	—	0.
10	1	0	942.42117	—	—	10	0	0	963.33775	—	—	0.17E+02
10	2	0	941.92323	—	—	10	0	0	963.23132	—	—	0.71E+02
10	3	0	940.86752	—	—	10	0	0	963.03897	—	—	0.35E+01
10	4	0	939.47981	—	—	10	0	0	962.79162	—	—	0.35E+01
10	5	0	937.13208	937.13190 (50) ^c	-18	10	0	0	962.44956	—	—	0.63E+01
10	6	0	935.22146	935.22160 (50) ^c	13	10	0	0	962.14466	—	—	0.22E+00
10	7	0	932.23491	—	—	10	0	0	961.77625	—	—	0.19E+00
10	8	0	928.59790	928.59810 (50) ^c	20	10	0	0	961.41104	—	—	0.32E+00
10	9	0	924.07034	—	—	10	0	0	961.08067	—	—	0.11E+01
10	10	0	916.62058	916.62090 (40) ^c	31	10	0	0	960.89230	960.89232 (20) ^a	2	0.94E+00
11	0	0	944.18216	—	—	11	0	0	962.01493	—	—	0.
11	1	0	943.97890	—	—	11	0	0	962.05139	—	—	0.55E+03
11	2	0	943.92577	—	—	11	0	0	962.54080	—	—	0.23E+02
11	3	0	942.56672	—	—	11	0	0	962.12081	—	—	0.11E+01
11	4	0	941.23902	—	—	11	0	0	962.05090	—	—	0.11E+01
11	5	0	939.49713	—	—	11	0	0	961.71423	—	—	0.21E+01
11	6	0	937.26876	—	—	11	0	0	961.32135	—	—	0.71E+01
11	7	0	934.48631	—	—	11	0	0	960.89324	—	—	0.63E+01
11	8	0	931.06222	—	—	11	0	0	960.44829	—	—	0.10E+00
11	9	0	926.89461	—	—	11	0	0	960.01903	960.01990 (20) ^a	-3	0.35E+00
11	10	0	921.81251	921.81200 (60) ^c	-50	11	0	0	959.58253	—	—	0.30E+00
11	11	0	915.46735	—	—	11	0	0	959.40783	—	—	0.53E+00
12	0	0	945.97850	—	—	12	0	0	962.01493	—	—	0.
12	1	0	945.97469	—	—	12	0	0	961.97266	—	—	0.10E+03
12	2	0	944.99563	—	—	12	0	0	961.86276	—	—	0.65E+03
12	3	0	944.13773	—	—	12	0	0	961.67016	—	—	0.34E+02
12	4	0	942.53994	—	—	12	0	0	961.32133	—	—	0.34E+02
12	5	0	941.32342	—	—	12	0	0	960.95300	—	—	0.51E+02
12	6	0	939.23701	—	—	12	0	0	960.51079	—	—	0.21E+01
12	7	0	936.47800	—	—	12	0	0	960.06272	—	—	0.18E+01
12	8	0	933.50828	—	—	12	0	0	959.51390	—	—	0.31E+01
12	9	0	929.64225	—	—	12	0	0	958.96929	—	—	0.10E+00
12	10	0	924.35002	924.34990 (100) ^a	-11	12	0	0	958.49673	—	—	0.80E+01
12	11	0	919.26078	—	—	12	0	0	958.08904	—	—	0.10E+00
12	12	0	912.38627	—	—	12	0	0	957.83021	—	—	0.56E+00
13	0	0	947.00895	—	—	13	0	0	961.93219	—	—	0.
13	1	0	946.87279	—	—	13	0	0	961.36274	—	—	0.53E+04
13	2	0	946.03115	—	—	13	0	0	961.20943	—	—	0.19E+03
13	3	0	945.72815	—	—	13	0	0	960.83489	—	—	0.93E+03
13	4	0	944.54977	—	—	13	0	0	960.61802	—	—	0.93E+03
13	5	0	943.05958	—	—	13	0	0	960.21266	—	—	0.17E+02
13	6	0	941.14816	—	—	13	0	0	959.74863	—	—	0.50E+02
13	7	0	939.77072	—	—	13	0	0	959.28281	—	—	0.50E+02
13	8	0	935.85017	—	—	13	0	0	958.61728	—	—	0.84E+02
13	9	0	932.59225	—	—	13	0	0	958.08942	—	—	0.25E+01
13	10	0	927.67693	—	—	13	0	0	957.39875	—	—	0.24E+01
13	11	0	922.75268	—	—	13	0	0	956.84111	—	—	0.82E+01
13	12	0	916.42842	—	—	13	0	0	956.13509	—	—	0.13E+00
13	13	0	908.76757	—	—	13	0	0	956.15139	956.15080 (70) ^a	-50	0.14E+00

In Eqs. (18)–(22), $m = 0$ for the ground state and $m = 1$ for the ν_2 state; the upper indices s and a denote respectively the lower and upper component of the inversion doublet; ΔE_m in Eq. (21) is defined as $\Delta E_m = E_m^{(a)} - E_m^{(s)}$, i.e., as the inversion splitting for $J = K = 0$ in the ground state ($m = 0$) and in the upper state ($m = 1$).

We introduce also the vector of the $\Delta k = \pm 3n$ interaction parameters [see

TABLE IV—Continued

J	K	C	$\sigma_R(J, K)$			$\sigma_R(J, K)$		
			O	(O-C)	I	C	O	(O-C)
				$\times 10^5$				$\times 10^5$
0	0	951.77627			0.32E+01	1 987.89921		0.
1	0	971.76107			0.	1007.94712		0.60E+01
1	1	971.88204	971.88204(10) ⁸	-1	0.23E+01	1007.94632		0.73E+01
2	0	991.60978			0.70E+01	1027.02280		0.
2	1	991.65030			0.34E+01	1027.04708	1027.04670(50)E	-33 8.94E+01
2	2	991.69053			0.23E+01	1027.07129	1027.07100(50)E	55 0.22E+01
3	0	1011.42788			0.	1046.40952	1046.40900(60)E	8 0.77E+01
3	1	1011.77554			0.37E+01	1046.40059	1046.40000(50)E	21 0.37E+01
3	2	1011.84514			0.31E+01	1046.36083	1046.36120(40)E	6 0.31E+01
3	3	1011.20366	1011.20350(10) ⁷	-16	0.40E+01	1046.37468	1046.37450(20)E	-18 0.40E+01
4	0	1031.28478			0.60E+01	1065.59021		0.
4	1	1031.60278			0.21E+01	1065.59432	1065.59440(50)E	7 0.31E+01
4	2	1031.31179			0.31E+01	1065.56172	1065.56200(50)E	67 0.10E+01
4	3	1031.21302			0.31E+01	1065.56352	1065.56300(50)E	-2 0.50E+01
4	4	1031.62237			0.10E+01	1065.56395	1065.56340(50)E	-25 0.13E+01
5	0	1051.13302			0.	1084.62902	1084.62960(60)E	58 0.51E+01
5	1	1051.01262			0.26E+01	1084.62370	1084.62440(60)E	70 0.23E+01
5	2	1051.25275			0.25E+01	1084.60901	1084.61020(50)E	18 0.24E+01
5	3	1051.12045			0.46E+01	1084.59313	1084.59300(20)E	-6 0.45E+01
5	4	1051.51198			0.19E+01	1084.59363	1084.59371(10)E	8 0.19E+01
5	5	1051.36037			0.12E+01	1084.59027	1084.59024(10)E	-2 0.12E+01
6	0	1071.09311			0.35E+01	1103.49166		0.
6	1	1071.42304			0.17E+01	1103.48393	1103.48440(60)E	57 0.17E+01
6	2	1071.20329	1071.20240(200) ⁸	-88	0.17E+01	1103.46982	1103.47000(70)E	58 0.17E+01
6	3	1071.41924			0.33E+01	1103.44128	1103.44130(60)E	22 0.13E+01
6	4	1071.62735			0.16E+01	1103.43030	1103.43110(60)E	59 0.15E+01
6	5	1071.59104	1071.59090(50) ⁸	-13	0.17E+01	1103.41923	1103.41940(60)E	-12 0.13E+01
6	6	1071.79745			0.17E+01	1103.47952	1103.48020(40)E	68 0.17E+01
7	0	1091.60920			0.	1122.10562	1122.10580(100)E	10 0.21E+01
7	1	1091.40014			0.11E+01	1122.17858	1122.17810(100)E	-58 0.10E+01
7	2	1091.11306	1091.11320(50) ⁸	13	0.11E+01	1122.14021	1122.14030(60)E	9 0.10E+01
7	3	1091.22936			0.21E+01	1122.13320	1122.13320(70)E	0 0.21E+01
7	4	1091.71136	1091.71190(50) ⁸	40	0.10E+01	1122.10886	1122.10820(50)E	13 0.10E+01
7	5	1091.61177			0.17E+01	1122.09371	1122.09370(70)E	-1 0.30E+00
7	6	1091.30996			0.17E+01	1122.11774	1122.11801(70)E	36 0.17E+01
7	7	1091.30417			0.50E+00	1122.20835	1122.20830(100)E	74 0.57E+00
8	0	1111.60846			0.11E+01	1140.70821		0.
8	1	1111.65977			0.37E+00	1140.70833		0.55E+00
8	2	1111.62750			0.50E+00	1140.67779		0.56E+00
8	3	1111.61999			0.10E+01	1140.66771		0.11E+01
8	4	1111.70678			0.60E+00	1140.60402		0.50E+00
8	5	1111.94938			0.00E+00	1140.57816		0.50E+00
8	6	1111.60878			0.10E+01	1140.57923		0.11E+01
8	7	1107.64943			0.52E+00	1140.62210		0.51E+00
8	8	1107.32246			0.36E+00	1140.77054		0.36E+00
9	0	1131.25849			0.	1159.00736		0.53E+00
9	1	1131.07878			0.20E+00	1159.04855		0.27E+00
9	2	1131.59326			0.20E+00	1159.02686		0.27E+00
9	3	1131.70851			0.50E+00	1159.08509		0.50E+00
9	4	1131.55690			0.30E+00	1159.02951		0.30E+00
9	5	1131.96656			0.32E+00	1159.08766		0.31E+00
9	6	1131.80976			0.05E+00	1159.06562		0.04E+00
9	7	1129.26179			0.31E+00	1159.08490		0.32E+00
9	8	1126.02915			0.36E+00	1159.07591		0.50E+00
9	9	1122.05560	1122.05550(70) ⁸	47	0.17E+01	1159.17992		0.12E+00
10	0	1151.66951			0.24E+00	1177.22954		0.42E+00
10	1	1151.64915			0.12E+00	1177.21989		0.12E+00
10	2	1151.08078			0.10E+00	1177.19761		0.12E+00
10	3	1151.30536			0.26E+00	1177.11153		0.25E+00
10	4	1151.20012			0.14E+00	1177.07850		0.13E+00
10	5	1151.74120			0.15E+00	1177.02165		0.14E+00
10	6	1151.82922			0.30E+00	1176.97486		0.30E+00
10	7	1151.07923			0.17E+00	1176.96363		0.16E+00
10	8	1147.52263			0.17E+00	1177.00845		0.17E+00
10	9	1142.90798			0.32E+00	1177.14777		0.32E+00
10	10	1139.66603			0.12E+00	1177.03180		0.12E+00
11	0	1171.63579			0.	1195.22011		0.92E+01
11	1	1171.66372			0.40E+01	1195.21003		0.47E+01
11	2	1171.28036			0.50E+01	1195.19632		0.40E+01
11	3	1171.59373			0.10E+00	1195.13613		0.10E+00
11	4	1171.61078			0.50E+01	1195.04752		0.54E+01
11	5	1171.28741			0.60E+01	1194.97671		0.50E+01
11	6	1171.58354			0.13E+00	1194.91114		0.13E+00
11	7	1171.52994			0.71E+01	1194.84770		0.71E+01
11	8	1168.77928			0.79E+01	1194.86936		0.77E+01
11	9	1165.50255			0.17E+00	1194.94778		0.16E+00
11	10	1161.40329			0.01E+01	1195.24645		0.00E+00
11	11	1156.56197			0.62E+01	1195.52897		0.61E+01
12	0	1191.71660			0.34E+01	1213.02517		0.
12	1	1191.54008			0.17E+01	1213.01362		0.17E+01
12	2	1191.21364			0.10E+01	1213.01791		0.12E+01
12	3	1191.62073			0.38E+01	1212.90402		0.37E+01
12	4	1191.75053			0.20E+01	1212.91893		0.20E+01
12	5	1191.53646			0.22E+01	1212.74856		0.22E+01
12	6	1191.01194			0.50E+01	1212.60467		0.48E+01
12	7	1191.09365			0.21E+01	1212.59403		0.27E+01
12	8	1189.71186			0.32E+01	1212.55686		0.31E+01
12	9	1181.77625			0.71E+01	1212.57999		0.69E+01
12	10	1183.17176			0.39E+01	1212.70800		0.39E+01
12	11	1178.75233			0.39E+01	1212.93887		0.38E+01
12	12	1173.33667			0.61E+01	1213.04104		0.60E+01
13	0	1213.27703			0.	1230.03659		0.11E+01
13	1	1213.04332			0.57E+02	1230.02511		0.55E+02
13	2	1217.02456			0.59E+02	1230.06930		0.57E+02
13	3	1217.27184			0.13E+01	1230.05933		0.13E+01
13	4	1216.45945			0.60E+02	1230.02603		0.60E+02
13	5	1215.44823			0.79E+02	1230.03162		0.77E+02
13	6	1215.09534			0.17E+01	1230.03122		0.16E+01
13	7	1212.39315			0.96E+02	1230.13132		0.95E+02
13	8	1210.27957			0.11E+01	1230.06624		0.11E+01
13	9	1207.67350			0.26E+01	1230.04001		0.25E+01
13	10	1204.47091			0.19E+01	1230.07161		0.19E+01
13	11	1200.33933			0.17E+01	1230.02544		0.16E+01
13	12	1195.71096			0.39E+01	1230.02612		0.38E+01
13	13	1189.77445			0.14E+01	1231.24038		0.14E+01

Eqs. (8)–(13)]

$$X_m^{(3n)} = \alpha_m, \beta_m, \eta_3^{(m)}, \eta_6^{(m)}. \quad (23)$$

We can now write in a symbolic form the following equations which specify the molecular parameters which can be determined from the individual types of experimental data:

$$\nu_{\text{inv}}^{(m)}(\Delta v_2 = 0; \Delta J = 0, \Delta K = 0, s \leftrightarrow a) = f(\Delta X_m, X_m^{(3n)}; X_m^{(JK)}, X_m^{(K)})$$

$$(m = 0, 1), \quad (24)$$

$$\nu_{\text{inv-rot}}^{(m)}(\Delta v_2 = 0; \Delta J = \pm 1, \Delta K = 0; s \leftrightarrow a) = f(\Delta X_m, X_m^{(J)}, X_m^{(JK)}; X_m^{(3n)}, X_m^{(K)})$$

$$(m = 0, 1), \quad (25)$$

$$\nu_2(\Delta v_2 = 1; \Delta J = 0, \Delta K = 0; s \leftrightarrow a) = f(X_1^{(J)} - X_0^{(J)}, X_1^{(JK)} + X_0^{(JK)}, X_1^{(K)} - X_0^{(K)}, E_1^s - E_0^s;$$

$$X_1^{(3n)}, X_0^{(3n)}, X_0^{(JK)}, X_0^{(K)}, X_1^{(JK)}, X_1^{(K)}), \quad (26)$$

$$\nu_{\text{rot}}^{(m)} \left[\Delta v_2 = 0; \Delta J = 0, \Delta K = \pm 3; \left(\frac{s}{a} \right) \leftrightarrow \left(\frac{s}{a} \right) \right]$$

$$= f(X_m^{(3n)}, X_m^{(JK)}, X_m^{(K)}; \Delta X_m) \quad (m = 0, 1), \quad (27)$$

$$\nu_{\text{rot}}^{(1)} \left[\Delta v_2 = 0; \Delta J = \pm 1, \Delta K = \pm 3; \left(\frac{s}{a} \right) \leftrightarrow \left(\frac{s}{a} \right) \right]$$

$$= f(X_1^{(3n)}, X_1^{(J)}, X_1^{(JK)}, X_1^{(K)}; \Delta X_1). \quad (28)$$

TABLE V

Wavenumbers (cm^{-1}) and Intensities ($\text{cm}^{-2} \text{atm}^{-1}$) of Perturbation-Allowed Transitions
 $\Delta K = \pm 3$ in $^{14}\text{NH}_3^a$

Transition	ν_{calc}	ν_{obs}	$\nu_{\text{obs}} - \nu_{\text{calc}}$	$I (\text{cm}^{-2} \text{atm}^{-1})$
Ground State Transitions				
$s(3,0) \leftarrow s(3,3)$	33.37620	-	-	1.1×10^{-7}
$s(4,0) \leftarrow s(4,3)$	33.20594	-	-	3.8×10^{-7}
$s(5,0) \leftarrow s(5,3)$	33.12502	-	-	3.5×10^{-7}
$s(6,0) \leftarrow s(6,3)$	32.91007	32.9090(20)	-0.0011	1.1×10^{-6}
$s(7,0) \leftarrow s(7,3)$	32.77081	32.7703(10)	0.0004	1.4×10^{-6}
$s(8,0) \leftarrow s(8,3)$	32.51804	32.5169(20)	0.0009	1.2×10^{-6}
$s(9,0) \leftarrow s(9,3)$	32.32134	- ^b	-	9.5×10^{-7}
$s(10,0) \leftarrow s(10,3)$	32.03079	32.0324(20)	0.0016	5.9×10^{-7}
ν_2 State Transitions				
$s(3,0) \leftarrow s(3,3)$	35.69689	35.69692(3)	0.00003	3.5×10^{-4}
$s(4,0) \leftarrow s(4,3)$	33.40704	-	-	1.7×10^{-9}
$s(5,0) \leftarrow s(5,3)$	35.31966	-	-	3.1×10^{-6}
$s(6,0) \leftarrow s(6,3)$	33.16092	-	-	5.8×10^{-9}
$s(7,0) \leftarrow s(7,3)$	34.79394	-	-	8.9×10^{-7}
$s(3,3) \leftarrow s(2,0)$	25.77095	25.77099(3)	0.00004	9.9×10^{-5}
$\Delta K = \pm 3$ Transitions in the ν_2 Band ^c				
$s(-3)Q(3,3)$	967.25016	967.2502(10)	0.0000	2.8×10^{-1}
$s(-3)Q(4,3)$	999.55543	-	-	2.0×10^{-6}
$s(-3)Q(5,3)$	969.02201	969.0210(30)	-0.001	2.5×10^{-3}
$s(-3)Q(6,3)$	998.29327	-	-	6.6×10^{-6}
$s(-3)Q(7,3)$	971.29885	-	-	7.4×10^{-4}

^aGround state and ν_2 state transitions wavenumbers taken from our measurements; $\Delta K = \pm 3$ transitions in the ν_2 band see ref. (16); values in parentheses of ν_{obs} are estimated experimental uncertainties in units of the last digit quoted.

^bBlended by H_2O absorption.

^c $s(-3)Q(J,K)$ means a ν_2 transition from the ground state J,K level with $\Delta J = 0, \Delta K = -3, (-3, \frac{1}{2}) \leftrightarrow (-3, \frac{3}{2})$.

TABLE VI

Ground-State and ν_2 -Excited State Molecular Parameters of $^{14}\text{NH}_3$ (cm^{-1})^a

Parameter	Ground-State Value	ν_2 -State Value	Parameter	Ground-State Value	ν_2 -State Value
ΔE_0	0.7934084(24)	35.688107(17)	(s) E_0	0	932.43384(13) ^c
ΔB	-5.05353(19)10 ⁻³	-0.1801512(41)	(s) B	9.9466429(59)	10.0701789(82)
$\Delta(C-B)$	7.05281(30)10 ⁻³	0.2516660(76)	(s) $C - (s)B$	-3.718280(24)	-3.981008(18)
ΔD_J	-1.67879(49)10 ⁻⁵	-0.43378(15)10 ⁻³	(s) D_J	0.84953(46)10 ⁻³	1.13076(57)10 ⁻³
ΔD_{JK}	4.6327(13)10 ⁻⁵	1.18809(41)10 ⁻³	(s) D_{JK}	-1.5783(16)10 ⁻³	-2.4226(15)10 ⁻³
ΔD_K	-3.17515(97)10 ⁻⁵	-0.80621(37)10 ⁻³	(s) D_K	1.0107(18)10 ⁻³	1.6172(19)10 ⁻³
ΔH_{JJJ}	-0.38725(51)10 ⁻⁷	-0.6094(18)10 ⁻⁶	(s) H_{JJJ}	0.2578(42)10 ⁻⁶	0.5577(92)10 ⁻⁶
ΔH_{JJK}	1.5834(19)10 ⁻⁷	2.4355(73)10 ⁻⁶	(s) H_{JJK}	-0.906(16)10 ⁻⁶	-2.221(37)10 ⁻⁶
ΔH_{JKK}	-2.1493(23)10 ⁻⁷	-3.205(11)10 ⁻⁶	(s) H_{JKK}	1.078(25)10 ⁻⁶	2.904(67)10 ⁻⁶
ΔH_{KKK}	0.9665(12)10 ⁻⁷	1.3877(66)10 ⁻⁶	(s) H_{KKK}	-0.200x10 ⁻⁶ ^b	-1.010(34)10 ⁻⁶
ΔG_{JJJJ}	0.6320(23)10 ⁻¹⁰	0.4321(69)10 ⁻⁹	(s) G_{JJJJ}	-0.116(10)10 ⁻⁹	-0.246(40)10 ⁻⁹
ΔG_{JJJK}	-3.434(11)10 ⁻¹⁰	-2.192(39)10 ⁻⁹	(s) G_{JJJK}	0.565(50)10 ⁻⁹	1.33(26)10 ⁻⁹
ΔG_{JJKK}	7.008(19)10 ⁻¹⁰	4.056(90)10 ⁻⁹	(s) G_{JJKK}	-1.069(88)10 ⁻⁹	-2.59(70)10 ⁻⁹
ΔG_{JJKKK}	-6.314(18)10 ⁻¹⁰	-3.23(11)10 ⁻⁹	(s) G_{JJKKK}	0.929(87)10 ⁻⁹	2.15(72)10 ⁻⁹
ΔG_{KKKK}	2.1129(70)10 ⁻¹⁰	0.920(57)10 ⁻⁹	(s) G_{KKKK}	-0.0333x10 ⁻⁹ ^b	-0.35(26)10 ⁻⁹
ΔL_{JJJJ}	-0.5489(38)10 ⁻¹³	0 ^b	η_3^o	4.2958(64)10 ⁻⁹	3.54(62)10 ⁻⁹
ΔL_{JJJK}	3.777(22)10 ⁻¹³	0 ^b	η_3^j	-5.571(75)10 ⁻¹²	-2.3(11)10 ⁻¹¹
ΔL_{JJKK}	-10.516(54)10 ⁻¹³	0 ^b	η_3^j	2.89(22)10 ⁻¹⁵	6.1(49)10 ⁻¹⁴
ΔL_{JJKKK}	14.496(75)10 ⁻¹³	0 ^b	η_6	-3.26(72)10 ⁻²⁰	0 ^b
ΔL_{JKKKK}	-9.846(51)10 ⁻¹³	0 ^b	ω	8.01(27)10 ⁻⁵	12.810(36)10 ⁻⁵
ΔL_{KKKKK}	2.639(15)10 ⁻¹³	0 ^b			

^a Values in parentheses are standard deviations of the parameters, given in units of the last digit quoted. ^b Constrained value. ^c Band origin for the $s \rightarrow a$ transition is 968.12195(13), for the $a \rightarrow s$ transition 931.64043(13) cm^{-1} .

It is obvious from Eqs. (24) that the same vector of molecular parameters may occur in different equations [for example, ΔX_m in Eqs. (24), (25), and (27)]. This illustrates the importance of a simultaneous least-squares fit to all the experimental data. Besides this, individual experimental data provide, in general, information of different quality for the determination of molecular parameters, either because of differences in their experimental accuracy or because individual parameters are more or less sensitive to these data. This is automatically taken into account during the iterational procedure described above [cf. Eqs. (14)–(17)], either in the process of formation of the whole Jacobian matrix, or by statistical weights assigned to individual experimental data.

If a symbol of molecular parameter is written before the semicolon in the right-hand sides of Eqs. (24)–(28), the corresponding experimental data provide “strong” information on this parameter; if it is written behind the semicolon, only “weak” information is obtained on the parameter. For example, the “perturbation-allowed” transitions [Eqs. (27)–(28)] provide “strong” information on the parameters $X_m^{(K)}$ [Eq. (20)] while only “weak” information is involved in the experimental data on the transitions obeying the usual selection rules [cf. also Ref. (2)].

Calculations have been done with the CDC Cyber 172 computer using double-precision arithmetic (120 bits). Excepting the ground-state inversion frequencies, the statistical weights assigned to the experimental data were $w_{pq} = \delta_{pq}^{-2}$, where δ_{pq} is the estimated uncertainty of the measurement (Tables I–V). The ground-state inversion frequencies were weighted as having $\delta = 0.05$ MHz although they have been mostly measured with better accuracy (3, 4). This was because our theoretical

model does not describe the hyperfine splittings of the rotational levels of ammonia. A value of the speed of light of $c = 299\,792.458\text{ km sec}^{-1}$ was used in converting the wavenumber units into frequency units.

Because the fitted parameters are in general correlated, considerable care had to be taken to use suitable damping factors during the first cycles of iteration in order to reach the convergence region where the damping factor could be put equal to zero.

IV. RESULTS AND DISCUSSION

The values of the transition frequencies, calculated from the converged set of molecular parameters in Table VI are compared with the experimental data in Tables I–V. In the last column of Tables I–V, the calculated intensities of the corresponding spectral lines are given. The intensities were calculated for $T = 300\text{ K}$ by standard methods (20) using Boltzmann factors and taking into account spatial degeneracy and spin statistical weights. The intensities of the “perturbation-allowed” transitions (Table V) were calculated from the coefficients of the mixing of the corresponding wavefunctions. The J, K dependence of the transition moments for the inversion–rotation and inversion transitions in the ground and ν_2 state of $^{14}\text{NH}_3$ has been taken from the paper of Shimoda *et al.* (21). The transition moments obtained by Špirko (22) have been used for the inversion–rotation transitions in the ν_2 band.

It is obvious from Tables I–V that we arrived at a quantitative description of the experimental data. The “smoothed” values of the transition frequencies are believed to be so accurate that $^{14}\text{NH}_3$ could now be used for calibration purposes in the far-infrared region and especially in the $10\text{-}\mu\text{m}$ region in diode laser spectroscopy. We believe that the precision of our calculated ν_2 -band wavenumbers in Table IV is better than 0.0015 cm^{-1} for transitions to the upper state $J' < 10$.

The standard deviation of the calculated ground-state inversion frequencies was 0.16 MHz . These microwave inversion frequencies have been described with an agreement slightly worse than 0.05 MHz assigned to these data in our theoretical treatment (Part III). The accuracy of our description of the ground-state microwave inversion frequencies is certainly sufficient for the purpose of the present work. Our fit in this respect represents the best description of these data based on a “physical” approach.

Molecular parameters obtained in our work (Table VI) can be considered to be the most precise parameters for the ground and ν_2 states of $^{14}\text{NH}_3$ published so far. In this respect one must mention the recently published impressive work of Shimoda *et al.* (21) on the infrared laser Stark spectroscopy of the ν_2 band of ammonia. These authors did not publish the “field-free” transition frequencies in their paper but only the values of molecular parameters. There is an excellent agreement between both papers as for the values of the ν_2 band origin and the ν_2 state parameters ΔX_1 [Eq. (21)]. However, there are differences between the values of other parameters beyond the quoted standard deviations. The reason for this seems to lie in the way in which Shimoda *et al.* (21) analyzed their excellent experimental

data. These authors have limited their considerations of the $\Delta k = \pm 3$ interactions to few rotational levels instead of considering sufficiently large interaction matrices. An extension of our simultaneous analysis to their data is possible, although not simple, and it should confirm our preliminary conclusions.

One of the ultimate goals in studying the vibrational-rotational states of ammonia is the determination of the energy levels of ammonia. The calculated intensities of the "perturbation-allowed" transitions in Table V indicate why it is so difficult to observe their lines in the ground and ν_2 states [except those in the ν_2 state which have enhanced intensities due to a close coincidence between the (3, 3) and (3, 0) levels, cf. Ref. (2)].

Although we have been able to assign certain extremely weak lines in the sub-millimeterwave spectra to the "perturbation-allowed" transitions in the ground state of ammonia (cf. Fig. 6 and Table V), they are of the same type as the previously detected transitions (2, 16) and the determination of a sufficiently complete set of spectroscopically "forbidden" parameters for ammonia has not yet been possible. The solution of this problem seems to be more promising by studying the perturbation-allowed transitions in the infrared $2\nu_4$ band of ammonia (23).

RECEIVED: December 4, 1980

REFERENCES

1. Š. URBAN, V. ŠPIRKO, D. PAPOUŠEK, R. S. MCDOWELL, N. G. NERESON, S. P. BELOV, L. I. GERSHTEIN, A. V. MASLOVSKIJ, A. F. KRUPNOV, J. CURTIS, AND K. NARAHARI RAO, *J. Mol. Spectrosc.* **79**, 455-495 (1980).
2. S. P. BELOV, L. I. GERSHTEIN, A. F. KRUPNOV, A. V. MASLOVSKIJ, Š. URBAN, V. ŠPIRKO, AND D. PAPOUŠEK, *J. Mol. Spectrosc.* **84**, 288-304 (1980).
3. R. L. POYNTER AND R. K. KAKAR, *Astrophys. J. Suppl. Ser.* **29**, 87-96 (1975).
4. B. V. SINHA AND P. D. P. SMITH, *J. Mol. Spectrosc.* **80**, 231-232 (1980).
5. P. HELMINGER, F. C. DE LUCIA, AND W. GORDY, *J. Mol. Spectrosc.* **39**, 94-97 (1971).
6. A. F. KRUPNOV, L. I. GERSHTEIN, V. G. SHUSTROV, AND V. V. POLYAKOV, *Radiofizika* **12**, 1584-1586 (1969).
7. S. M. FREUND AND T. OKA, *Phys. Rev. A* **13**, 2178-2190 (1976).
8. H. JONES, *Appl. Phys.* **15**, 261-264 (1978).
9. T. KOSTIUK, M. J. MUMMA, J. J. HILLMAN, D. BUHL, L. W. BROWN, J. L. FARIS, AND D. L. SPEARS, *Infrared Phys.* **17**, 431-439 (1977).
10. J. M. DOWLING, *J. Mol. Spectrosc.* **27**, 527-538 (1968).
11. J. KAUPPINEN, *Appl. Opt.* **18**, 1788 (1979).
12. M. CARLOTTI, A. TROMBETTI, B. VELINO, AND J. VRBANCICH, *J. Mol. Spectrosc.* **83**, 401-407 (1980).
13. A. F. KRUPNOV AND A. V. BURENIN, in "Molecular Spectroscopy: Modern Research" (K. Narahari Rao, Ed.), Vol. 2, Academic Press, New York, 1976.
14. S. P. BELOV, A. V. BURENIN, L. T. GERSHTEIN, V. V. KOROLICHIN, AND A. F. KRUPNOV, *Opt. Spectrosc. (USSR)* **35**, 295-302 (1973).
15. S. P. BELOV, L. I. GERSHTEIN, AND A. V. MASLOVSKIJ, Proceedings of the Vth All-Union Symposium on Molecular Spectroscopy of High and Superhigh Resolution, Tomsk-Novosibirsk, 1980.
16. D. LAUGHTON, S. M. FREUND, AND T. OKA, *J. Mol. Spectrosc.* **62**, 263-270 (1976).

17. E. N. KARYAKIN, A. F. KRUPNOV, D. PAPOUŠEK, JU. M. SHCHURIN, AND Š. URBAN, *J. Mol. Spectrosc.* **66**, 171–173 (1977).
18. F. Y. CHU AND S. M. FREUND, *J. Mol. Spectrosc.* **48**, 183–184 (1973).
19. D. PAPOUŠEK, S. TOMAN, AND J. PLIVA, *J. Mol. Spectrosc.* **15**, 502–505 (1965).
20. W. GORDY AND R. L. COOK, "Microwave Molecular Spectra," Interscience, New York/London/Sydney/Toronto, 1970.
21. K. SHIMODA, Y. UEDA, AND J. IWAHORI, *App. Phys.* **21**, 181–189 (1980).
22. V. ŠPIRKO, *J. Mol. Spectrosc.* **74**, 456–464 (1979).
23. R. J. NORDSTROM, T. K. BALASUBRAMANIAN, K. NARAHARI RAO, AND R. PAPOUŠEK, Thirty-Fifth Symposium on Molecular Spectroscopy, The Ohio State University, Columbus, Ohio, 1980.
24. N. NERESON, *J. Mol. Spectrosc.* **69**, 489–493 (1978).
25. H. JONES, In "Proceedings Vth Internat. Seminar on High Resolution Infrared Spectroscopy, Liblice near Prague, 18–22, Sept. 1978."